Diploma Thesis

Are the current radiological parameters to evaluate the growing hip still up-to-date?

submitted by

Sophie Butter

for the Academic Degree of

Doktor(in) der gesamten Heilkunde

(Dr. med. univ.)

at the

Medical University of Graz

conducted at

Division of Paediatric Orthopaedics

under the Supervision of

Ass.-Prof. Priv.-Doz. Dr.med.univ. Tanja Kraus

Univ.FA Priv.-Doz. Dr.med.univ. Dr.scient.med. Sebastian Tschauner

Dr.med.univ. Dr.scient.med. Thomas Zwetti

Graz, 29.11.2021

Statutory Declaration

I declare on my word of honour that I have written the present work independently and without the help of others, that I have not used any sources other than those indicated and that I have marked the passages taken from the sources used, either literally or in terms of content.

Graz, 29.11.2021 *Sophie Butter eh.*

Acknowledgements

I would like to thank my my supervisors Ass.-Prof. Priv.-Doz. Dr.med.univ. Tanja Kraus, Univ. FA Priv.-Doz. Dr.med.univ. Dr.scient.med. Sebastian Tschauner and Dr.med.univ. Dr.scient.med. Thomas Zwetti for their guidance and their constant availability in case of any questions and uncertainties. They have guided me through the challenges of this thesis with commitment, professional expertise and relentless support.

Then I would like to thank my parents Ursula and Walter from the bottom of my heart. They have always been there for me with their unconditional love and support. Without them, studying medicine would not have been possible.

The biggest thanks goes to my better half, Maximilian. With his support and encouragement, I was able to bring out the best in me in this diploma thesis.

THANK YOU!

TABLE OF CONTENTS

List of Abbreviations

A.	Arteria
Aa.	Arteriae
AC	Acetabular
Art.	Articulatio
CE	Center-Edge
CP	Cerebral Palsy
ECF	Epiphysiolysis Capitis femoris
Lig.	Ligamentum
M.	Musculus
Mb.	Morbus
MI	Migration Index (according to Reimer)
N.	Nervus
R.	Ramus
V.	Vena

List of Figures

List of Tables

Zusammenfassung

Einleitung: Ziel dieser Arbeit war es, zu klären, ob die bis dato verwendeten radiologischen Parameter zur Beurteilung der wachsenden Hüfte noch aktuell sind. Die hierzu aktuell existierenden Normwerte, die an einer sehr kleinen PatientInnengruppe erhoben wurden und weiterhin im täglichen Gebrauch eines Kinderorthopäden sind, sind schon mehrere Jahrzehnte alt. Es wurden daher aktuelle Röntgenbilder (Beckenübersicht) der kindlichen Hüfte altersgestaffelt vermessen, mit den existierenden und im klinischen Alltag verwendeten Hüftparametern (Acetabulumwinkel, Centrum-Ecken-Winkel, Reimers Migrationsindex) verglichen und in ihrer Aktualität überprüft.

PatientInnen und Methoden: In die Studie eingeschlossen wurden PatientInnen zwischen 0 und 18 Jahren, die eine gesunde Hüfte vorwiesen. Zur Datenerhebung wurden bereits existierende Beckenübersichtsaufnahmen von 3786 PatientInnen, welche zwischen 2006 und 2018 durchgeführt wurden, verwendet. Insgesamt 1774 Röntgenbilder für die weitere Auswertung geeignet. Die Berechnung der hüftspezifischen Parameter erfolgte am Computer mit Hilfe der Bildanalyseplattform „Supervisely“. Dafür wurden Kennpunkte am Röntgenbild eingezeichnet und nach Abschluss der Markierungen automatisiert ausgelesen. Die anschließende Datenanalyse erfolgte mittels deskriptiver Statistik.

Ergebnisse: Nach Abschluss des Selektionsprozesses verblieben insgesamt 1774 Röntgenbilder zur weiteren Auswertung, von denen 666 weiblichen und 1108 männlichen PatientInnen zugeordnet werden konnten. Das Durchschnittsalter der Mädchen lag bei 9,11 Jahren, während die Buben durchschnittlich 9,28 Jahre alt waren. Sowohl der Acetabulumwinkel als auch der Centrum-Ecken-Winkel zeigten sich nach ihrer Berechnung vergleichbar mit den bereits existierenden Daten. Die Winkel jeder Altersgruppe fielen in die bisher existierende Normgröße und konnten daher als physiologisch eingestuft werden. Auch beim Reimers Migrationsindex lagen die Werte in allen außer zwei Altersgruppen innerhalb der physiologischen Norm (0-10%). Bei den Altersgruppen "15 - 15,99 Jahre" und "16 - 16,99 Jahre" kam es zu einer Überschreitung des Grenzwertes von 0,1% und 0,3% nach oben.

Schlussfolgerung: Die vorliegende Diplomarbeit bestätigt, dass die bis dato verwendeten radiologischen Parameter zur Beurteilung des wachsenden Hüftgelenks im Hinblick auf den Acetabulumwinkel und den Centrum-Ecken-Winkel nach wie vor aktuell sind und für den klinischen Alltag weiterhin herangezogen werden sollen. Die Ergebnisse von Reimers Migrationsindex zeigten sich in zwei Altersgruppen minimal erhöht. In den übrigen Altersklassen konnte der Migrationsindex jedoch als physiologisch eingestuft werden. Somit ist auch die Anwendung des Migrationsindex im klinischen Alltag weiterhin empfohlen.

Abstract

Background: The aim of this diploma thesis was to answer whether the current radiological parameters to evaluate the growing hip are still up-to-date. The currently existing values, which were collected from a very small group of patients and are still in daily use by pediatric orthopedists, are already several decades old. The purpose of this work is to measure current pelvic radiographs of the pediatric hip according to age, compare them with existing hip parameters used in clinical practice (acetabular angle (AC angle), center-edge angle (CE angle), Reimer's migration index (MI)) and to evaluate the validity of this data.

Patients and Methods: All patients between 0 and 18 years of age who presented with a healthy hip were included in the study. Existing pelvic radiographs of 3786 patients, acquired between 2006 and 2018, were used for data collection. A total of 1774 radiographs were suitable for further evaluation. To calculate the hip-specific parameters, key points were marked on X-ray images on a computer using the image analysis platform "Supervisely", which automatically determined the parameters after completion of the markings. The following data analysis was performed using descriptive statistics.

Results: After completion of the selection process, a total of 1774 radiographs remained for further evaluation, of which 666 could be assigned to female and 1108 to male patients. The average age of the girls was 9,11 years, while the average age of the boys was 9,28 years. After their calculation, both the acetabular angle and the center-edge angle were found to be comparable to the existing data. The angles of each age group were within the given norm and could therefore be classified as physiological. In all but two age groups, the values of Reimer's migration index were within the physiological norm (0-10%). There was a exceedance of the threshold of 0,1% and 0,3% upwards in the age groups "15 - 15,99" and "16 – 16,99".

Discussion: The present study confirms that the current radiological parameters to evaluate the growing hip regarding the acetabular angle and the center-edge angle are still valid and should maintain their use in clinical practice. Reimer's migration

index scores were slightly elevated in two age groups. This can be further clarified in a study with a larger number of patients. However, for the remaining age groups, the migration index was found to be physiological, implying that the use of the migration index remains relevant in the clinical setting.

1 Introduction

In daily clinical practice, many different parameters are used to assess various health conditions. In the field of radiology, many of these parameters are based on X-ray images. The main focus is to find out whether the currently used radiological parameters for the assessment of the growing hip are still up-to-date.

1.1 Aim of the study

The main aim of this diploma thesis is to measure hip-specific parameters of the pediatric hip at different ages. A prerequisite for this is the presence of a healthy hip. After measurement, the values are compared with existing standard values used in everyday clinical practice. In general, these values are derived from the book “Normalwerte in Wachstum und Entwicklung" (translated: “Normal values in growth and development”) by C. Ulrich Exner (3). The standard values described by Exner are a compilation of several studies in which hip-specific parameters were examined. The studies show, that the existing data is several years old and were mostly collected from small groups of patients. It is controversial whether the existing data is representative of the standard values of the pediatric hip. The data evaluated in the practical part of this thesis should either confirm or invalidate the results obtained in the past.

1.2 Hypothesis

The following two hypotheses were created to define the main objective of the thesis.

Null hypothesis H_0:
During the measurement and evaluation of the hip-specific parameters, there is no change in the measured values compared to the standard values used up to now.

Alternative hypothesis H_1:
During the measurement and assessment of the hip-specific parameters, there is a change in the measured variables compared to the standard values used up to now.

2 Theoretical Principles – Anatomy of the hip joint

The following chapters describe the anatomy and development of the hip joint in detail.

2.1 Bones of the hip joint and bony structure

The hip joint (Articulatio (Art.) pubis forms the connection between the femur and the pelvis. While the Caput femoris and its Facies articularis form the joint head, the socket is built by the Acetabulum and its crescent-shaped Facies lunata. Basically, the hip joint connects the lower extremity with the trunk. Since the legs have primarily a supporting function, the joint socket is more robustly (4).

2.1.1 Hip socket

In the hip socket (Acetabulum) the Os pubis, the Os ilium and the Os ischii meet by forming a Y-shaped cartilage, the so-called triradiate cartilage. The acetabulum is surrounded by a discontinuous osseous rim, the Limbus acetabuli. The reason for the cleft in the rim is that the Limbus acetabuli is separated by an incision called Incisura acetabuli (5). At the bony edge of the Acetabulum lies the fibrocartilaginous Labrum acetabulare, which primarily serves to enlarge the surface of the socket articulating with the femoral head. The Labrum acetabulare makes it possible for the femoral head to be enclosed by the acetabular cup for more than two thirds (6). In the middle of the Acetabulum is a cavity, called the Fossa acetabuli. While the fossa itself is not involved in articulation, its crescent-shaped Facies lunata forms an important part of the joint surface. The Facies lunata receives its annular appearance because the Ligamentum (Lig.) transversum acetabuli connects both ends with each other. Beneath this ligament, blood vessels and nerves enter the acetabular fossa (7).

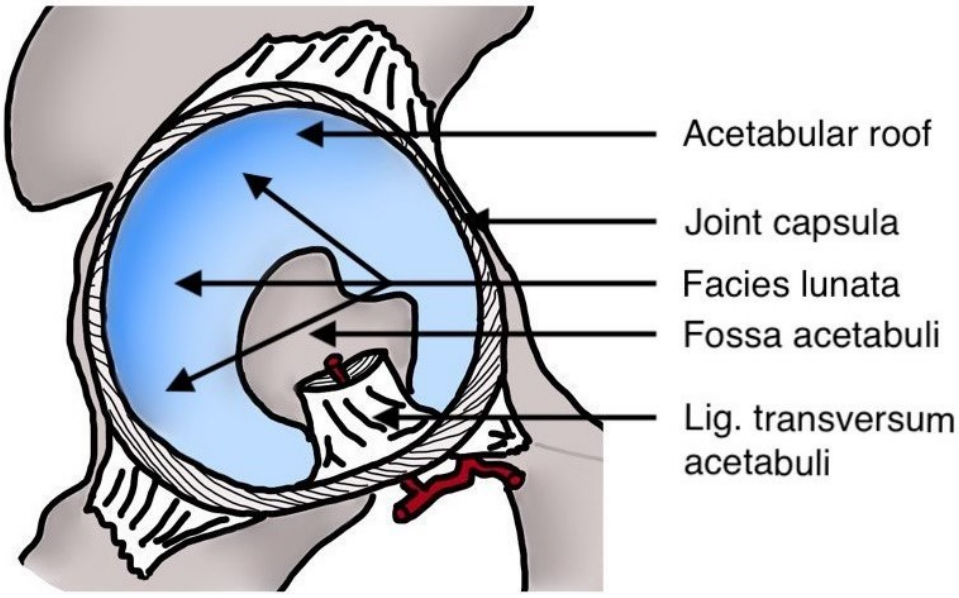

Figure 1: Acetabulum

This illustration represents the acetabulum from a lateral view. The joint capsule is opened and the ligaments are severed. Adopted with modification by (8).

2.1.2 Joint Head

The joint head is formed by the femoral head (Caput femoris), which appears nearly spherical and has a small, non-cartilaginous pit on top called the Fovea capitis. Originating from the Fovea the Lig. Capitis femoris extends to the acetabular fossa, which is located at the centre of the socket. The cartilaginous surface of the femoral head appears as a wide convex ring, which decreases in thickness in the periphery (9). The arterial supply to the joint head is discussed in more detail in chapter 2.7 “Vascularisation”. For more information on when the Y-shaped cartilage is closed and the appearance of the ossification center, see chapter 3.2 “3.2Postnatal development”.

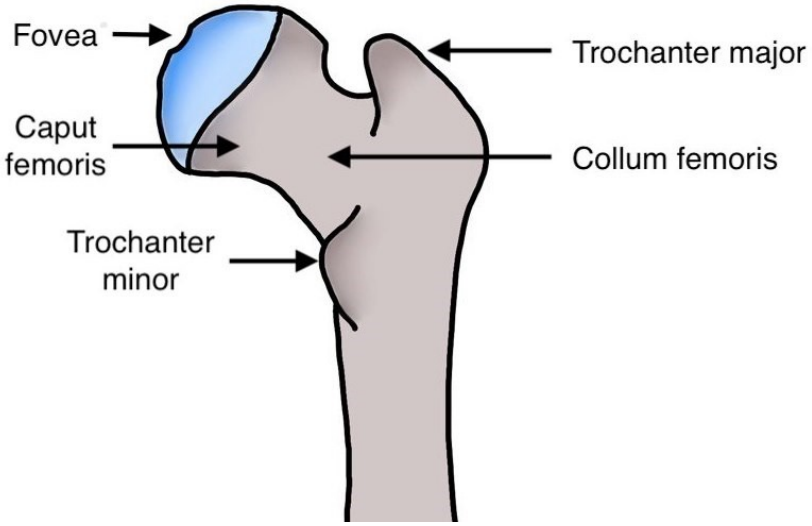

Figure 2: Proximal femur in dorsal plane

This image shows the proximal femur, which includes the femoral head, neck and the region 5cm distal to the lesser trochanter. It shows which area of the femoral head is involved in articulation. Adopted with modification by (10,11).

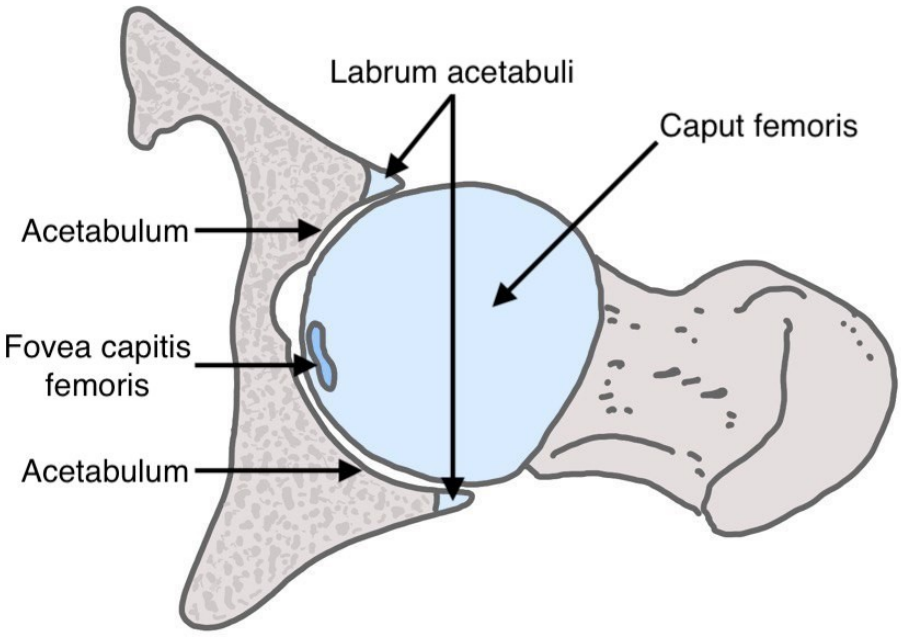

Figure 3: Caput femoris in transversal plane

This image represents how the articular surfaces of the femoral head and acetabulum interact with each other during articulation. Adopted with modification by (12).

2.1.3 Joint type

The hip joint can be considered an Art. simplex because its consistence of only two joint bodies. It represents a particular type of the ball joint (Art. spheroidea): the nut joint (Art. cotylica). The ball shaped joint head articulates with the spherical, concave joint socket. In doing so the acetabulum encloses the femoral head by almost two thirds. Movements in the hip joint are possible in all three directions. Due to these three degrees of freedom, the hip joint can perform flexion/extension, abduction/adduction and inner/outer rotational movements. There is also the possibility of performing circumduction in the hip joint, which is a combination of all three fundamental types of movement. Despite the ability of all degrees of freedom, there are restrictions of movement due to musculoskeletal structures and the capsule-ligament apparatus (7,13).

Using the neutral-zero method to measure the movements in the hip joint results in the following values (14):

Movement	**Radius of Movement**
Flexion / Extension	120-140 / 0 / 10
Adduction / Abduction	15-20 / 0 / 30-45
Internal Rotation / External Rotation (with extended hip joint)	36 / 0 /13
Internal Rotation / External Rotation (with flexion of the hip by 90°)	40-50 / 0 / 30-45

Table 1: Hip Joint movement with radius

This table represents the maximum range of motion in the hip joint. Adopted according to (14).

2.2 Joint capsula

The funnel-shaped capsule of the hip joint is the thickest capsule in the human body. It consists of two parts: the Membrana fibrosa and the Membrana synovialis (14,15).

The **Membrana fibrosa** forms the outer part of the joint capsule. It is a tight connective tissue originating from the bony edge of the Acetabulum, the Ligamentum transversum acetabuli and the outer edge of the Labrum acetabulare. The Membrana fibrosa inserts on the anterior and posterior side of the femur: anteriorly where the intertrochanteric line is located, posteriorly about 1,5cm proximal to the crista intertrochanterica (14,15).

The inner side of the capsule is covered by the **Membrana synovialis**. It originates at the Labrum acetabularis and extends to the bone-cartilage-line of the caput femoris. The Membrana synovialis plays an important role as it produces a fluid called synovia, which nourishes the joint cartilage (14,15).

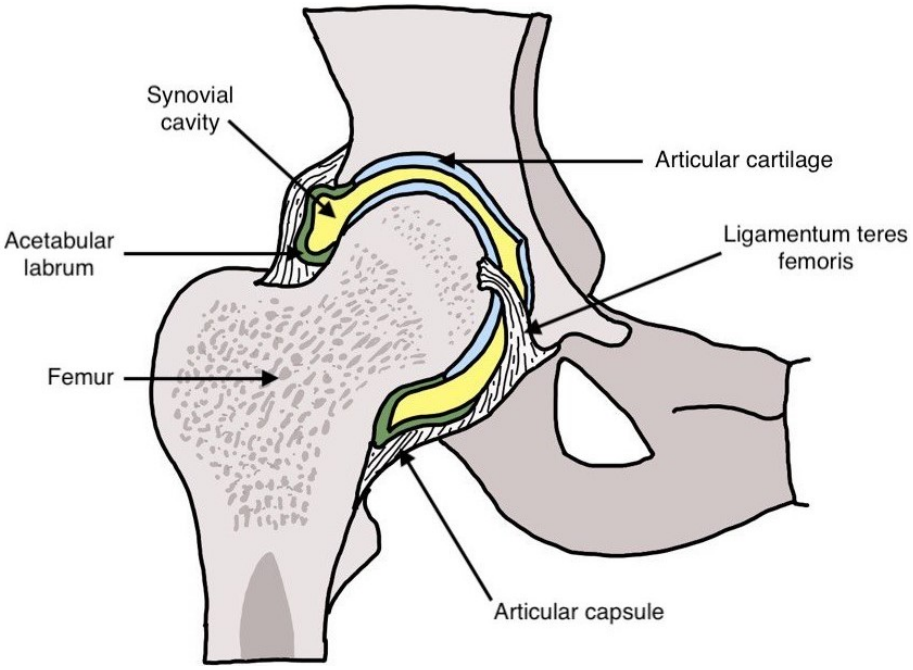

Figure 4: Cross section of the hip joint

This picture illustrates the hip joint in cross-section from a ventral perspective. The anatomical structures and the course of the capsule are visualized. Adopted with modification by (16).

2.3 Ligaments

Since the hip joint carries the entire body weight to the legs, it requires a strong ligamentous apparatus. These ligaments provide stable motion and prevent the pelvis from tilting dorsally by limiting the extension of the hip joint. Spirally wrapping around the femoral head and neck leads to a strong tension during extension. Between the ligaments of the hip joint, the capsule has weaker areas where traumatic dislocations can occur (14).

The following describes the various ligaments that are part of the hip joint. In addition, the upcoming figure shows the described ligaments:

- **iliofemoral ligament**: located between the Spina iliaca anterior inferior of the Os ilium to the Linea intertrochanterica of the femur
- **pubofemoral ligament**: located between the Eminentia iliopectinea and Crista obturatoria to the Linea intertrochanterica
- **ischiofemoral ligament**: located between the posterior edge of the Acetabulum and from Os ischii to the Linea intertrochanterica of the femur
- **orbicular zone**: contains fibres from all three bands mentioned above and runs in a ring around the collum of the femur

Among these, the iliofemoral ligament is the strongest ligament of the human body.

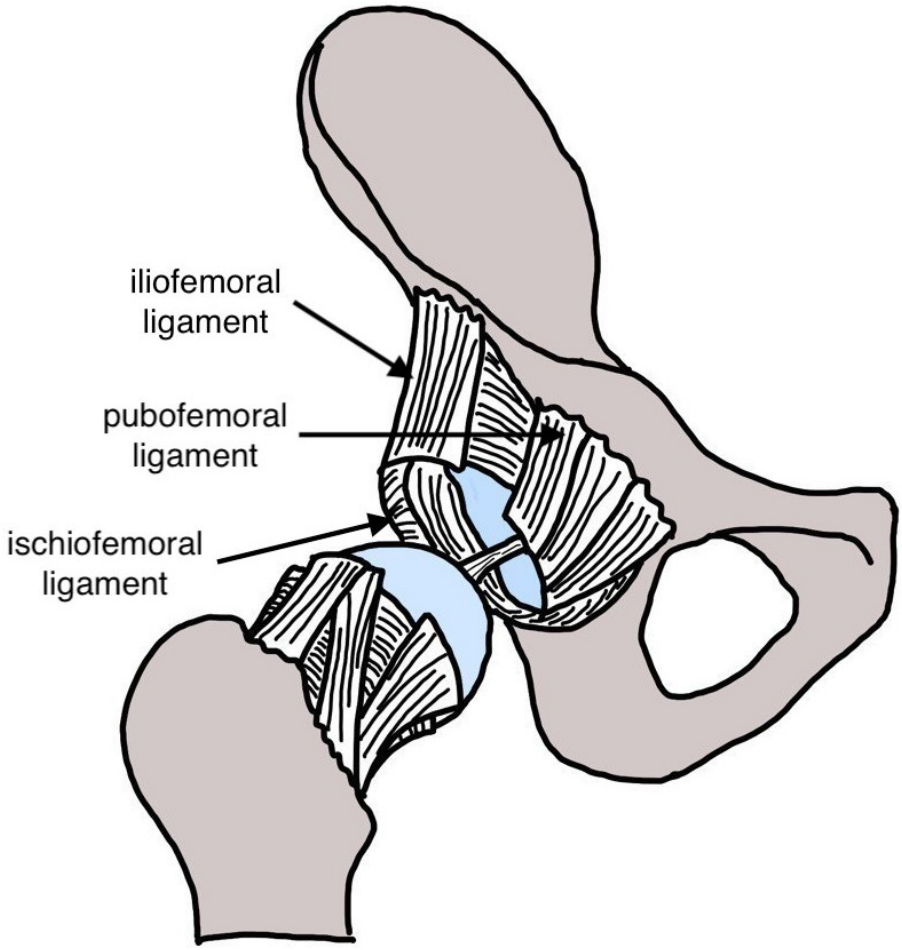

Figure 5: Ligaments of the hip joint

This image shows the three ligaments surrounding the hip joint. To show them all in one image, the ligaments have divided crosswise. Adopted with modification by (17).

There is a ligament inside the joint called Ligamentum capitis (teres) femoris. While it has no holding function, it is involved in the arterial supply of the femur, especially in children. The blood supply is maintained by the Arteria (A.) capitis femoris, which obliterates at about the age of 4 years (4).

2.4 Bursa

Below the M. iliopsoas, in the triangle between the Lig. iliofemorale and the Lig. pubofemorale, the Bursa iliopectinea is located. It supports the locomotor system in transmitting pressure and also helps to protect the capsule of the hip joint underneath (7,18).

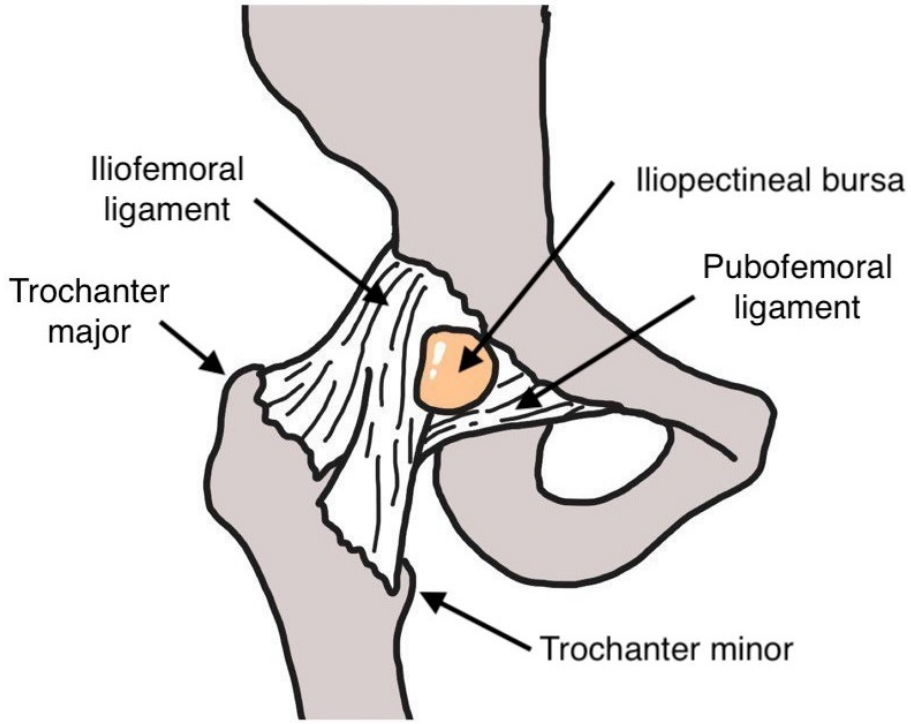

Figure 6: Bursa iliopectinea

This image shows the Bursa iliopectinea, which is located above the hip joint. It ensures frictionless mobility between the tendon of the M. iliopsoas and the hip bone. Adopted with modification by (19).

2.5 Muscles

To enable the body to stand, walk and move, the hip joint is surrounded by a large mass of muscles. Considering their main function, they can be categorised as flexors, extensors, abductors, adductors, external rotators and internal rotators (20,21).

Ventral muscles

The only muscle in this group is the Musculus (M.) iliopsoas, which consists of two parts: the M. iliacus and the M. psoas major (20,21).

Dorsolateral muscles

These muscles radiate from the outer surface of the wings of ilium (Alae ossis illi) to the area around the greater trochanter (Trochanter major) in a fan-shaped pattern.

The M. gluteus maximus plays a significant role in shaping the profile of the gluteal region while it is almost completely covering the other muscles. Ventrally and cranially, the M. gluteus medius extends by covering the M. gluteus minimus. Most lateral there is the M. tensor fasciae latae located, which later migrates into the Tractus iliotibialis (20,21).

Pelvitrochanteric muscles

As the muscles of the pelvitrochanteric group originate inside and at the edge of the lesser pelvis (Pelvis minor), they reach the outside where they blend with the aforesaid fan-shaped pattern of the dorsolateral muscles. The muscles involved are: the M. piriformis, M. triceps coxae, M. quadratus femoris and M. obturatorius externus (20,21).

Adductor muscles

The adductors originate at the pubic bone and the Tuber ischiadicum. Their origin extends from the lesser trochanter (Trochanter minor) along the Linea aspera to the Epicondylus medialis femoris and continues with the M. gracilis to underneath the medial head of the tibia. The M. gracilis is located most medially. From proximal to distal are the M. pectineus, M. adductor brevis, M. adductor longus and M. adductor magnus (20,21).

2.6 Nerves

Motor nerves transmit signals to the muscles. In this way, they cause the muscles to contract and enable movements in the joint.

The hip joint is innervated by the following motor nerves:

- femoral nerve (N. femoralis)
- obturator nerve (N. obturatorius)
- sciatic nerve (N. ischiadicus)
- inferior gluteal nerve (N. gluteus inferior)
- superior gluteal nerve (N. gluteus superior) (15)

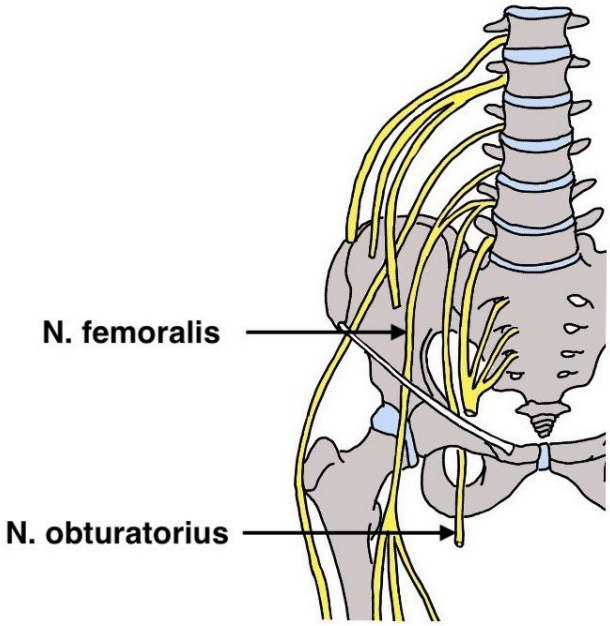

Figure 7: Nerves ventral

The illustration shows the motor innervation of the hip ventrally by showing the N. femoralis and N. obturatorius. Adopted with modification by (11).

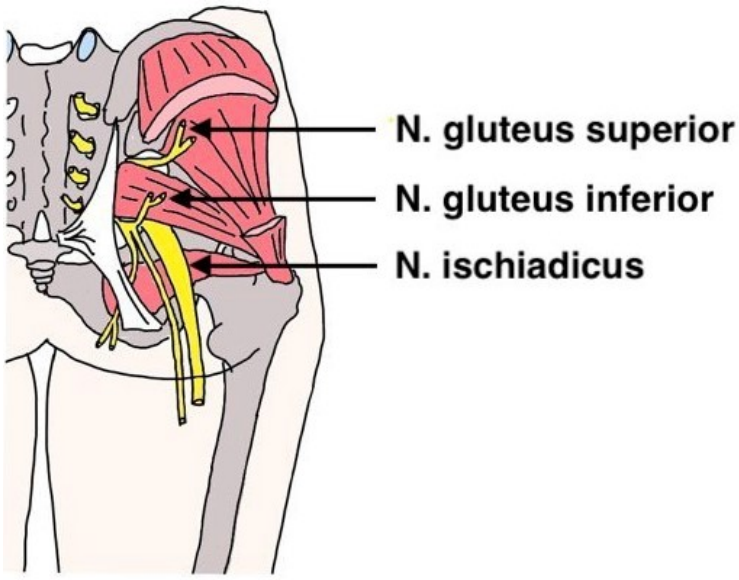

Figure 8: Nerves dorsal

The illustration shows the motor innervation of the hip dorsally by showing the N gluteus superior, N. gluteus inferior and N. ischadicus. Adopted with modification by (22).

2.7 Vascularisation

Caput femoris

The blood supply to the femoral head is mostly provided by:

- **A. circumflexa femoris lateralis** (originating from the A. femoralis profunda)
- **A. circumflexa femoris medialis** (originating from the A. femoralis profunda)

In that area a small branch from the obturatorial artery (Ramus (R.) acetabularis), which is also called A. capitis femoris, branches off to the ligament capitis femoris and partially supplies the caput femoris too. The A. capitis femoris is responsible for the femoral head supply in childhood. It obliterates in the 4th year of life. (15).

Acetabulum

The acetabulum is supplied by the following branches of the internal iliac artery (A. iliaca interna):

- **A. obturatoria**
- **A. glutea superior**
- **A. glutea inferior**
- **A. pudenda interna** (15)

3 Theoretical Principles – Development of the hip joint

In the following paragraphs, the development of the pediatric hip joint will be discussed in more detail. The focus here is primarily on prenatal and postnatal growth

3.1 Prenatal development

The extremities develop from the 4th week of pregnancy as buds of the lateral trunk wall. In the 6th week of pregnancy a hip system can already be seen and in the 8th week the joints are essentially developed and almost all joint components are

formed. At this time the pelvis consists of cartilage tissue in which three ossification centres (Os ilium, Os pubis and Os ischii) are formed. In the 3rd and 4th embryonic months, the ossification centers of these 3 bones are formed. These meet in the acetabulum during later development in a y-shaped fugue (23–25).

The ossification process is differentiated between primary and secondary ossification. Primary ossification refers to the initial formation of bone tissue, which leads to the formation of woven bone. As for secondary ossification, it describes the transformation of pre-existing bone into lamellar bone (26). Tubular bones are formed by enchondral ossification. This leads to the formation of bone, which progresses from the inside to the outside and consists of a cartilaginous intermediate stage. The ossification centres in the diaphysis are formed in the 12th week of pregnancy, followed by longitudinal growth of the tubular bones in the cartilaginous growth zone (27,28).

3.2 Postnatal development

At the time of birth, the diaphyses are mostly ossified. The epiphyses, on the other hand, have not developed ossification centres yet. Ossification of the proximal end of the femur originates from an epiphyseal nucleus in the region of the femoral head and from one in the region of the greater trochanter. While the epihyphyseal nucleus of the femoral head appears at 2-8 months of age, that of the greater trochanter occurs between 2 and 7 years of age (25). After nine months the ossification centre of the femoral head should be visible on a X-ray image. The distance between the diaphysis and the ossification centre of the epiphysis is called the epiphyseal plate, which has a central role in the longitudinal growth of the bones. As soon as the longitudinal growth of the bone has completed, the epiphyseal plate disappears and a bony connection between the epiphysis and the diaphysis is formed, leaving only an epiphyseal line. Fusion of the epiphyseal plate happens between 15 and 21 years of age in males, and between 14 and 19 years of age in females, after the trochanteric nuclei have merged with the ossification of the diaphysis and femoral neck (25).

Distal and proximal epiphyseal plates are involved in the overall length growth of tubular bones. The growth of the epiphyseal plates near the knee joint is greater than that of the joints far from the knee joint. At the lower extremity, 70% of the length growth is taken by the distal femoral epiphysis and 30% by the proximal femoral epiphysis (29). The following illustration shows the longitudinal growth just described.

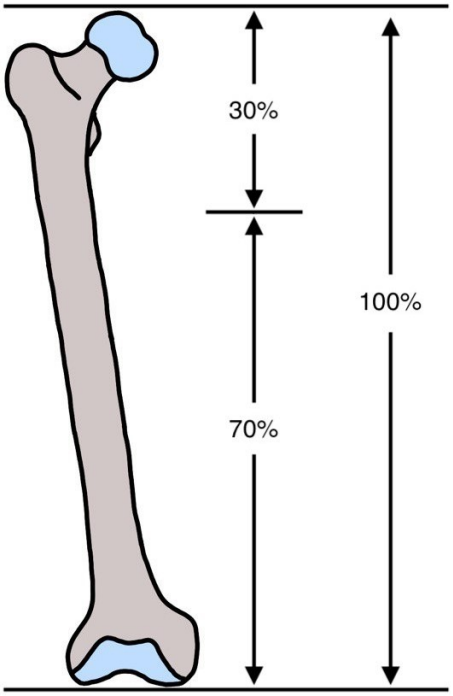

Figure 9: Longitudinal growth of the femur

This figure shows the proportions of the different growth zones of the femur. Adopted with modification by (30).

The study "Changes in the shape of the human hip joint during its development and their relation to its stability" by Z. Ralis and B. McKibbin shows that during embryonic development the acetabulum almost completely surrounds the femoral head (31). As pregnancy progresses, the acetabulum flattens and the femoral head gradually loses its globular character and takes on a hemispherical appearance until birth. Once the child is born, this process is reversed. The head of the femur becomes more spherical and the pelvic socket increases in depth again. This development is maintained throughout childhood and is a possible argument for the increased risk of dislocation of the child's hip (31).

4 Theoretical Principles – Hip specific parameters

In the following chapters, the hip-specific parameters referred to in this thesis are explained in more detail. In particular, four different measurements are referred to in these subsections:

- Center-edge angle
- Hilgenreiner's line
- Acetabular angle
- Reimer's migration index

4.1 Center-edge angle

The center-edge angle gives information about the coverage of the femoral head and about the position of the head within the acetabular cup. As this angle increases, the depth of the acetabulum increases too. If the angle decreases, the acetabulum gets more shallow and therefore more dysplastic. With normal hip development the CE angle typically gets larger with a person's age - in children up to 13 years of age it should be 20°, afterwards above 25°. Values below 20° suggest acetabular dysplasia (32,33). Measurement of the CE-angle requires the presence of an ossification center, which may be delayed and eccentric in the femoral head. The angle is less reliable the younger the child, since the acetabulum and proximal femur are still mostly cartilaginous (34).

To measure the CE angle, two lines need to be drawn. The first one runs straight from the centre of the femoral head to the outer edge of the superior acetabulum rim. The second one goes orthograde (= parallel to the longitudinal body-axis) through the centre of the femoral head. Once these two lines are intersected with each other, the CE angle can be calculated (6,35).

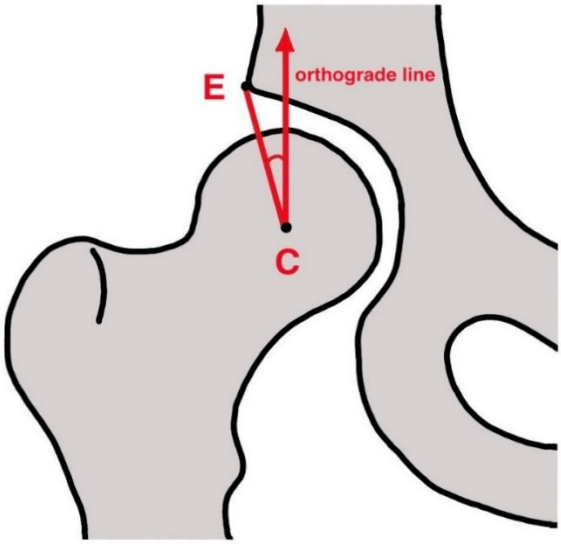

Figure 10: CE angle

This illustration shows how the CE angle is calculated. Therefore, an orthograde line is drawn through the centre of the femoral head and connected to the outer edge of the acetabulum. C = Center of the femoral head; vertical line through femoral head center. E = Edge of the superior acetabular rim. Adopted with modification by (36).

4.2 Hilgenreiner's line

The Os pubis, the Os ilium and the Os ischia meet in the center of the Acetabulum, where they are form a Y-shaped cartilage called the triradiate cartilage. The Hilgenreiner's line is defined as a horizontal line between the two Y-shaped cartilages of the right and left acetabulum. It is also necessary for calculating the AC angle (37).

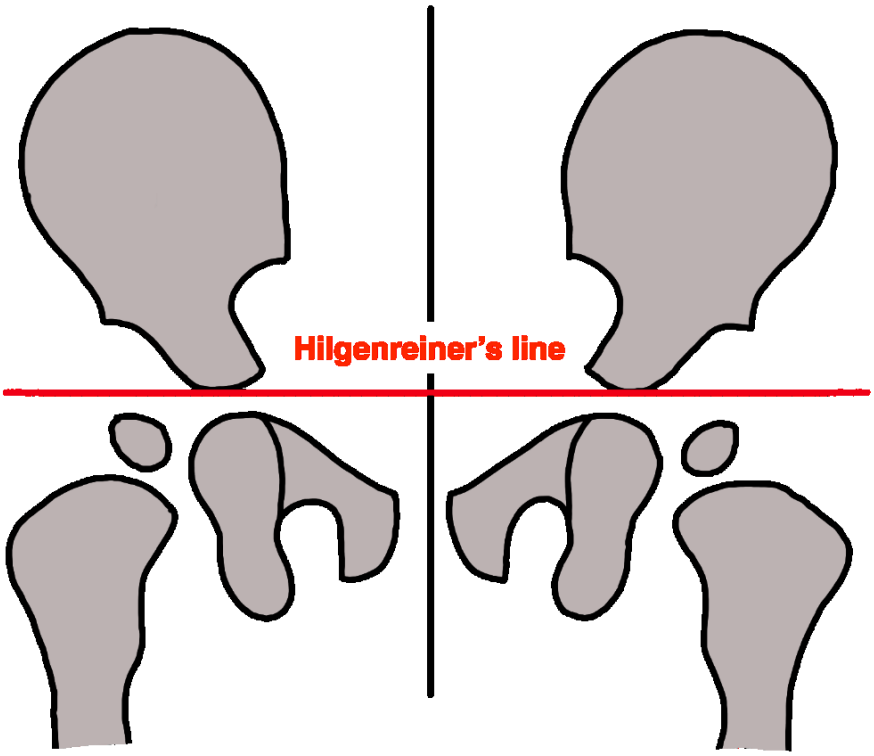

Figure 11: Hilgenreiner's line

This illustration shows the path of the Hilgenreiner's line. For this, a horizontal line is drawn through the two Y-shaped cartilages of the hip. Adopted with modification by (38).

4.3 Acetabular angle

The AC angle is used to evaluate the incline of the acetabulum in the case of congenital hip dislocation and the development of the child's hip joint in general (24,39). To measure the acetabular angle, a connecting line from the triradiate cartilage to the lateral edge of the acetabular roof is drawn. This line is then intersected with the Hilgenreiner's line. The resulting angle is called the AC angle (37,40). Measurement of the AC angle is only possible as long as the Y-shaped cartilage has not yet ossified. The closure of the Y-shaped cartilage should be completed by the age of 15, but often happens earlier.

The AC angle should be around 30° in the newborn, < 25° in the 1st year of life, < 23° in the 3rd year, < 20° in the 7th year, and < 15° in the 15th year (6).

If the AC angle is larger than it should be at this age, it leads to insufficient coverage of the femoral head and thereby promotes decentration of the hip. In acetabular dysplasia, there is abnormal development of the acetabulum. The femoral head does not find a firm hold in the acetabulum, therefore the risk of femoral head dislocation increases. The reason for this is that the angle is too large due to the flattening of the lateral edge of the acetabular roof. In consequence, there is inadequate coverage of the femoral head and the risk of decentration of the Caput femoris increases (40).

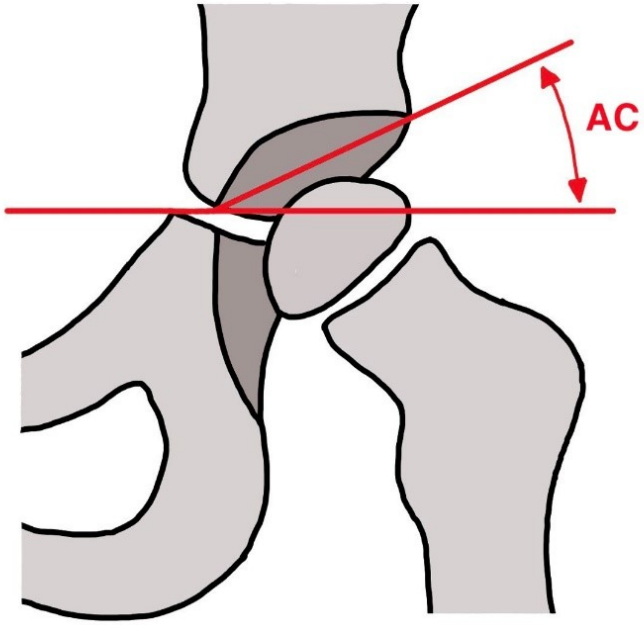

Figure 12: AC angle

This illustration shows the measurement of the AC angle. For this purpose, a line is drawn from the Y-shaped cartilage to the lateral edge of the acetabular roof. The angle between this line and the Hilgenreiner's line is called the AC angle. Adopted with modification by (41).

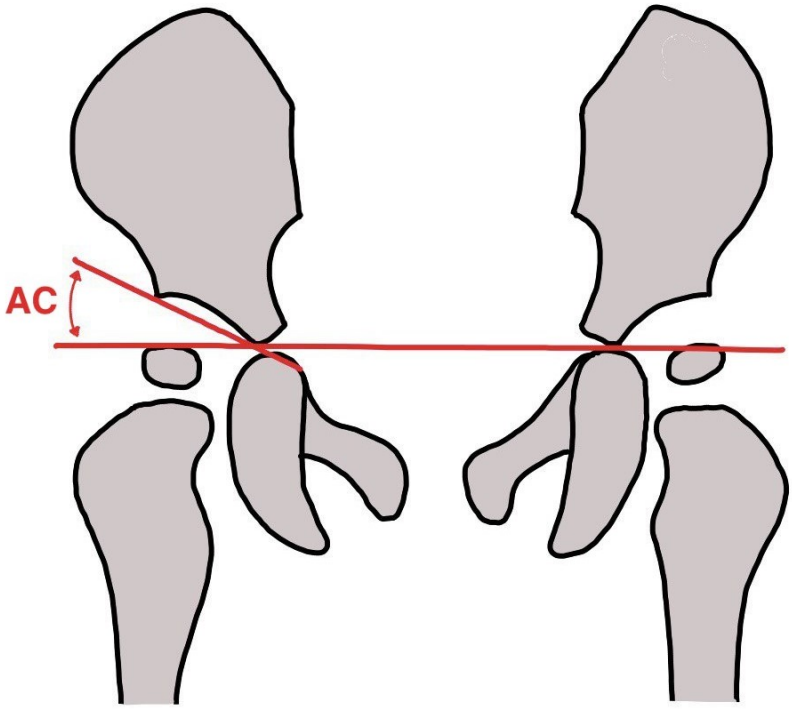

Figure 13: AC angle from a ventral perspective

This picture illustrates how the AC angle is measured in the pelvic X-ray. Here, one line runs through the lateral acetabular rim to the Y-shaped cartilage. Hilgenreiner's line is the line connecting the two Y-shaped cartilages. The AC angle is obtained by measuring the angle between these two lines. Adopted with modification by (42).

4.4 Reimer's migration index

The Reimer migration index measures the decentration of the femoral head and can be used to determine the level of lateralisation of the hip (43). It indicates the percentage of the femoral head covered by the outer edge of the acetabulum. Reimer's migration index is therefore used as a measure of head coverage (44). To calculate the migration index, a vertical line is drawn through both lateral and medial edges of the femoral head. In addition, a vertical line called the Ombrédanne-Perkins line is put through the most lateral point of the acetabular roof. The part of the femoral head located laterally of the acetabulum is marked as A and the part located medial of the acetabulum is marked as B (45). Figure 8 illustrates the calculation of the migration index of Reimer:

$$MI = \frac{A}{B} * 100\%$$

The migration index is calculated by dividing the part lateral to the Ombredanne-Perkins line by the total width of the femoral head. The result is then multiplied by 100. The resulting value is given as a percentage. In this context, 100% corresponds to a complete dislocation. Errors are caused by measurement variations, inaccurate measurements or inaccurate recordings. In particular, the accurate determination of the reference point is crucial for the measurement of the migration index (34).

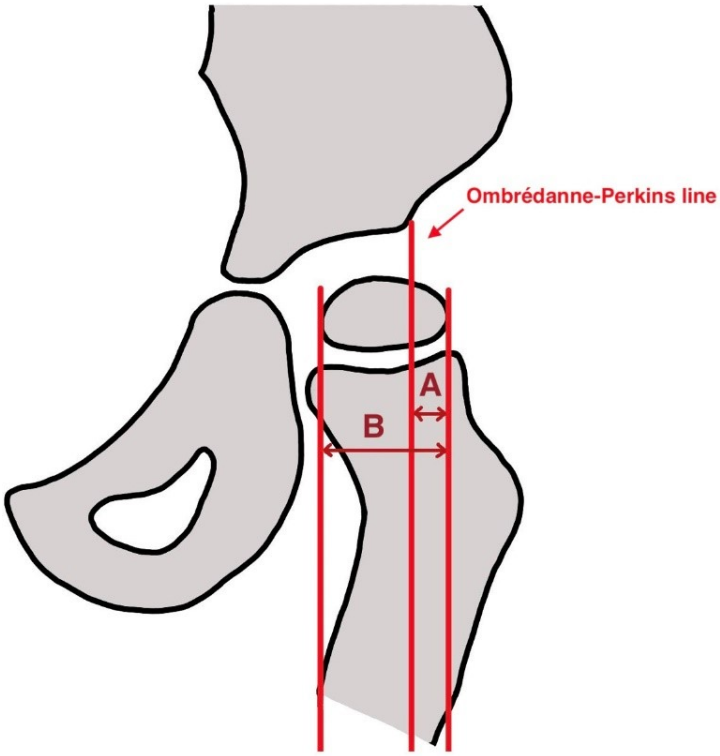

Figure 14: Reimer's migration index

To calculate the migration index, an orthograde (Ombredanne-Perkins line) is placed through the most lateral point of the acetabular roof. Then two vertical lines are drawn on both the lateral and medial borders of the femoral head. The distance of the femoral head lateral to the acetabular roof is named “A” and the distance medial to the femoral head is named “B”. Adopted with modification by (46).

5 Clinical practice – Reference values in use

The book "Normalwerte in Wachstum und Entwicklung" by C. Ulrich Exner (29) is frequently used in the clinical field. This book provides the current normal values and helps to identify deviations from the norm. Its data has been used worldwide for many years, as they originate from well-known and widely published studies (3). The following sections of this chapter present the results of the studies Exner used in his book. In addition, these values represent the reference values with which the data presented in this thesis are compared.

5.1 CE angle

For the comparison with the CE angles calculated in this thesis, two studies referenced in Exner (29), Scoles et al. (47) and Brückl (48), were referred to. In addition to Exner, Tönnis also published a study on CE angles in children in 1984 (49). The next three paragraphs describe the three different types of studies.

CE angle according to Scoles et al.

One requirement for calculating the CE angle is that sufficient ossification of the femoral head has already taken place. Therefore, it is difficult or even impossible to evaluate for children under two years of age. In 1987, the article "Roentgenographic parameters of the normal infant hip" was published by Peter Scoles (47). It indicates that in children up to two years, the ossification centre is used to calculate the CE angle instead of the actual femoral head centre (3).

For his study, hip joints of 50 girls and 50 boys at the age of 3, 6, 9, 12, 18 and 24 months were examined. With increasing age, an increase in the CE angle was also seen in both sexes. The mean value for girls at an age of 3 months was 18°, the mean value at an age of 24 months was 30°. For boys at 3 months of age it was 20° and increased to 24° at 24 months (47).

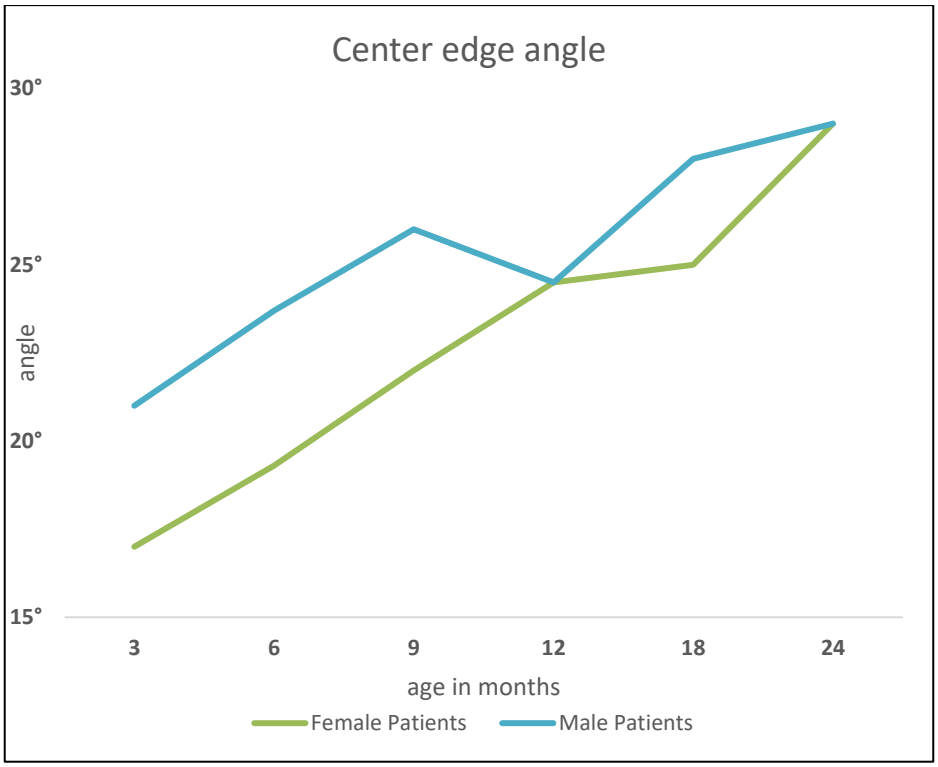

Figure 15: Normal values of the CE angle according to Scoles

This graph shows a gradual increase in the angle for both sexes in the time range from 3 to 24 months of age. Adopted with modification by (47).

CE angle according to Brückl

In 1979, Reinhard Brückl evaluated various parameters in X-ray images of children and adolescents aged 5 to 20 years (48). This also included the evaluation of the CE angle according to Wiberg's method. Since sufficient ossification of the femoral head can be assumed in this age group, the well-known CE angle by Wiberg is used. The CE angle is usually at least 15° in children and increases with age (48).

The following two charts show the results of Brückl's study:

Age (years)	Girls	Number	Boys	Number
5 + 6	23,5 ± 6,0	106	24,0 ± 6,6	80
7 + 8	26,5 ± 6,2	76	25,5 ± 6,0	64
9 + 10	30,5 ± 4,7	128	30,5 ± 4,6	60
11 + 12	32,7 ± 5,4	92	30,6 ± 4,7	46
13 + 14	34,2 ± 4,8	68	33,0 ± 6,3	66
15 + 16	34,9 ± 6,1	77	35,2 ± 4,9	43
17 + 18	33,5 ± 5,4	56	37,1 ± 6,0	38
19 + 20	35,5 ± 5,3	56	35,1 ± 4,3	54

Table 2: Mean values of the CE angle for both sexes

This table shows the mean values and the standard deviation of the CE angle by Wiberg for eight different age groups from 5 to 20 years. Adopted with modification by (48).

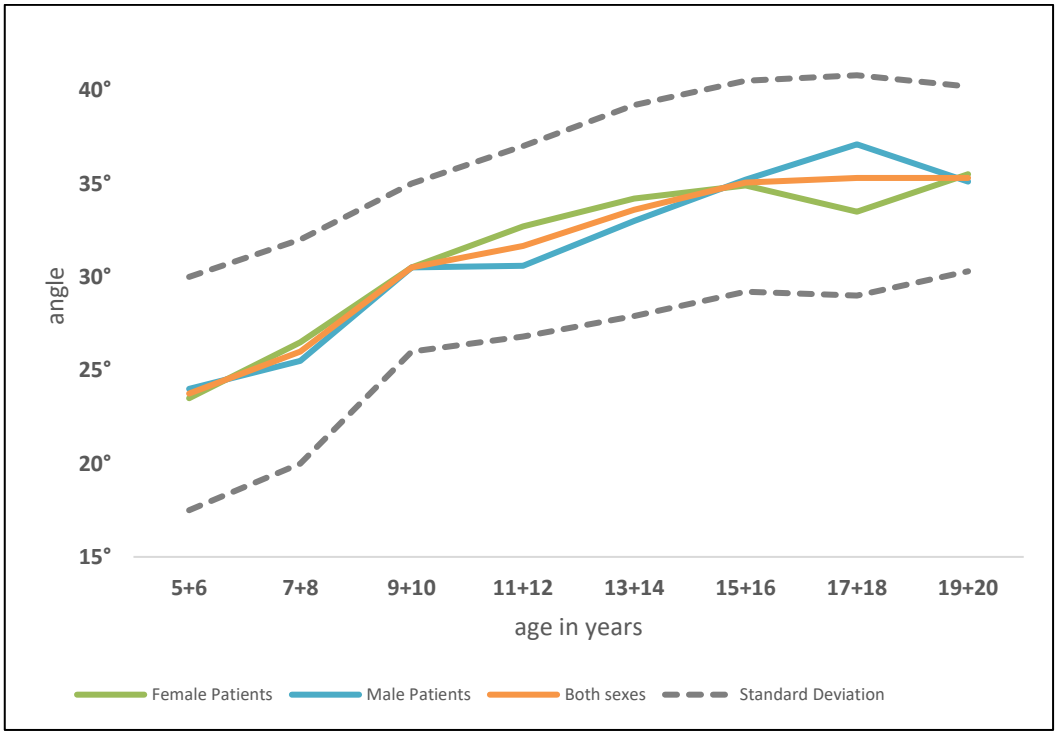

Figure 16: Plot of the mean values and standard deviation of the CE angle

This graph shows the mean values of the CE angle of girls and boys from 5 to 20 years. It also presents the standard deviation for the overall mean value. Adopted with modification by (48).

CE angle according to Tönnis

Tönnis published a study in 1984 in which he determined the CE angles of children and adults. His age intervals were set wider than Brückl's and he did not present his results in a gender-specific form (49).

The table below presents Tönnis' results and the degrees of deviation in the age groups from 0-8, 8-18 and 18-50:

Age (years)	Mean value	Grade I (normal)	Grade II (mildly pathological)	Grade III (severely pathological)	Grade IV (extremely pathological)
≥0 - ≤8	25	≥20	≥15 - <20	≥0 - <15	<0
≥8 - ≤18	32	≥25	≥20 - <25	≥5 - <20	<5
≥18 - 50	35	≥30	≥20 - <30	≥5 - <20	<5

Table 3: CE angle of both sexes from 0 to 50 years of age

This table shows the normal values of the CE angle divided into age groups from 0 to 50 years. Any deviations from the normal value are categorised into four groups, which are displayed from "normal" to "highly pathological". Adopted with modification by (49).

5.2 AC angle

In 1968, D. Tönnis and D. Brunken published their study "Eine Abgrenzung normaler und pathologischer Hüftpfannendachwinkel zur Diagnose der Hüftdysplasie" (translated: "A delineation of normal and pathologic acetabular roof angles for the diagnosis of hip dysplasia."), where the AC angle on 3164 hip joints from 1256 children at different ages were considered. Of these, 435 radiographs (870 hips) were not used. Therefore, 2294 hips remained, of which 1438 were assigned to female participants and 856 to male participants. 476 hip joints were checked more than once during the course of the study (50).

The following charts show Tönnis' results for the development of the AC angle:

Age (years/months)	Mean value	Grade I (normal)	Grade II (mildly pathological)	Grade III (severely pathological)	Grade IV (extremely pathological)
0/3 + 0/4	25	<30	≥30 - <35	≥35 - <40	≥40
0/5 – 2/0	20	<25	≥25 - <30	≥30 - <35	≥35
2 – 3	18	<23	≥23 - <28	≥28 - <33	≥33
3 – 7	15	<20	≥20 - <25	≥25 - <30	≥30
7 - 14	10	<15	≥15 - <20	≥20 - <25	≥25

Table 4: AC angle of both sexes from 0 to years of age

This table shows the normal values of the AC angle divided into age groups from 0 to 15 years. Any deviations from the normal value are categorised into four groups, which are displayed from "normal" to "highly pathological". Adopted with modification by (49) .

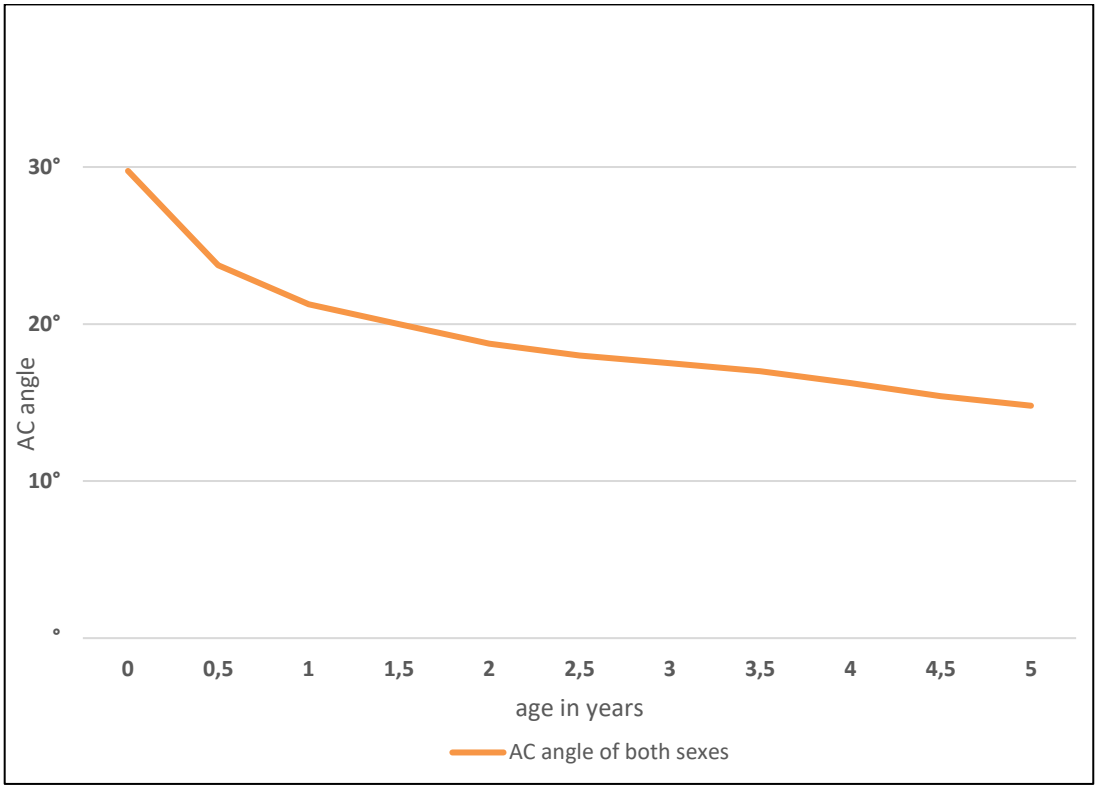

Figure 17: AC angle of children between the age of 0 and 5 years

This graph shows the mean values of the AC angle of children between 0 and 5 years of age. Adopted with modification by (37).

5.3 Reimer's migration index

The migration index was not included by Exner in his book. For reasons of clinical importance, it has been included in this thesis. An important tool for identifying decentration of the femoral head is the migration index according to Reimer. It indicates how much of the femoral head is located outside the acetabulum. The result is given as a percentage. Based on the MI, the hip can be classified into different degrees of dislocation (51).

Migration percentage (%)	Definition and progression
0 – 10	Normal
10 – 30	Mild subluxation
30 – 60	Moderate subluxation
60 – 90	Severe subluxation
> 90	Dislocated

Table 5: Reimer's migration index

This table represents the extent of lateralisation and dislocation of the femoral head in relation to the MI. Adopted according to (51).

6 Patient and methods

This chapter describes the procedure of the clinical trial.

6.1 Study design

This research represents a monocentric study with retrospective data analysis from an existing database, which was provided by the Department of Radiology of the State Hospital Graz. The included X-ray images are originated from patients treated at the Department of Pediatric and Adolescent Surgery of the Medical University of Graz between 2006 and 2018. The patient data were sourced from the documentation system “MEDOCS”, a communication and information network of KAGES (“Steiermärkische Krankenanstaltengesellschaft”). The pelvic X-ray images required for measurement were taken from a system for digital image archiving, distribution and processing (PACS).

6.2 Patient selection

For data evaluation pelvic overview images of 3786 patients within a range from of 0 to 18 years were used. In general, only x-rays of healthy children's hips were taken into analysis. After elimination of non-matching candidates, a total of 1774 suitable X-ray images remained for the evaluation of the pelvic X-ray images. The gender distribution of the included patients is random. Since both male and female patients were examined, the expected results are equally relevant for both sexes. Gender-specific characteristics found during the evaluation are presented separately.

Inclusion criteria:

- Patient age between 0 and 18 years
- Healthy children without underlying diseases affecting the hip
- Presence of at least one pelvic radiograph
- Presentation at the Peditaric center at the Medical University of Graz

Exclusion criteria:

- Patients > 18a
- Traumatic changes of the hip like fractures
- Pathological atraumatic changes of the hip as in Perthes disease, congenital hip luxations, epiphysiolysis capitis femoris (ECF), spastic cerebral palsy, spina bifida, systemic diseases involving the hip like Achondoplasia, epiphyseal dysplasia, or traumatic changes like fractures of the pelvic ring, acetabulum and femoral head.
- X-rays taken for follow-up
  (If several X-rays are available from one patient and the interval between these images was less than 6 months, the X-ray image that showed better image quality was used for the study. If the time interval between two X-ray images was too short, significant changes in the bony structures of the hip joint were not expected so that the x-ray was excluded.)
- Poorly adjusted X-ray images

6.3 Data collection

The following parameters were analysed:

- Age
- Gender
- Previous illnesses / injuries
- Medical findings of the present radiograph
- Date of the X-ray image(s)

Since the sole evaluation of the radiographs was inadequate for deciding which patients were included in the study, the computerised documentation system "MEDOCS" was used to receive information about any pre-existing conditions that might lead to exclusion from the study. It helped to obtain information about possible pre-existing conditions that could lead to exclusion from the study.

6.4 Radiological evaluation

Since the cartilaginous parts of the growing hip joint are larger in younger children, radiological tools must be used to analyse the hip-specific parameters. These are measured on the computer using the image analysis platform "Supervisely", which is licensed by the Clinical Department of Pediatric Radiology. After marking the required orientation points on the X-ray images, the programme is able to assess the absolute position of the tagged coordinates. Based on this, a CSV (comma separated value) file was exported. In this file, the angles between the marked positions were calculated using trigonometric functions in Microsoft® Excel.

To ensure a correct evaluation of the hip-specific parameters some criteria have to be considered while taking the X-ray image. For an explanation of the correct assessment of an X-ray image, see the following chapter 6.4.1.

6.4.1 Guidelines for the correct use of the X-Ray technology

When imaging the pediatric hip joint, special attention should be paid to the following aspects:

- Symmetrical positioning of the thighs in a standardised position
- Both halves of the pelvis and femoral necks should be exposed symmetrically and evenly
- The Trochanter major should not overlap the neck of the femur, while the Trochanter minor is just visible
- Both Foramina sacralia should appear symmetrical in the image
- Complete visualization of the triradiate cartilage
- Visualization of the periarticular soft tissue
- Radiation protection: testicle or ovarian protection

(52)

Assuming that the above conditions were met, the following hip-specific parameters were measured:

- AC angle and Hilgenreiner's line (see chapters 4.3 and 4.2)
- CE angle (see chapter 4.1)
- Reimer's migration index (see chapter 4.4)

6.4.2 Correct identification of the hip specific data points

The following chapters explain in more detail how to correctly measure the hip-specific angles.

The following X-ray image demonstrates the healthy hip joint of a five-year-old girl and serves as a reference model for measuring the various hip parameters. This X-ray image serves as a template to illustrate the positioning of the markings in the following chapters.

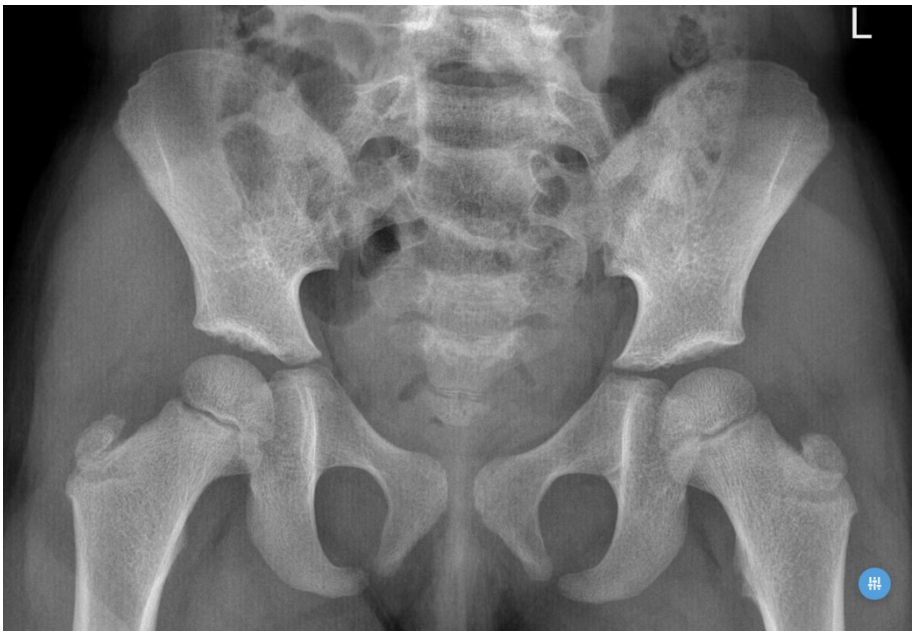

Figure 18: Plain X-ray of the hip

This image shows an X-ray of a 5-year old female patient. It demonstrates how the radiograph originally looked before the markings for calculating the AC angle, CE angle and MI were placed.

6.4.2.1 AC angle and Hilgenreiner's line

To calculate the AC angle, the outermost point of the acetabulum must be identified. Once this is done, the point is marked on the X-ray image using the web-based platform "Supervisely". Then, the most caudal point of the triradiate cartilage is identified and tagged in the X-ray image as well.

With these two points the AC angle can be calculated. The first line runs from the acetabular edge to the Y-joint, while the second line (=Hilgenreiner's line) runs horizontally through both triradiate cartilages. Identifying the Hilgenreiner's line is not always easy, as the triradiate cartilage begins to ossify at an age of 16 to 18 years, sometimes even earlier and cannot always be clearly identified (53).

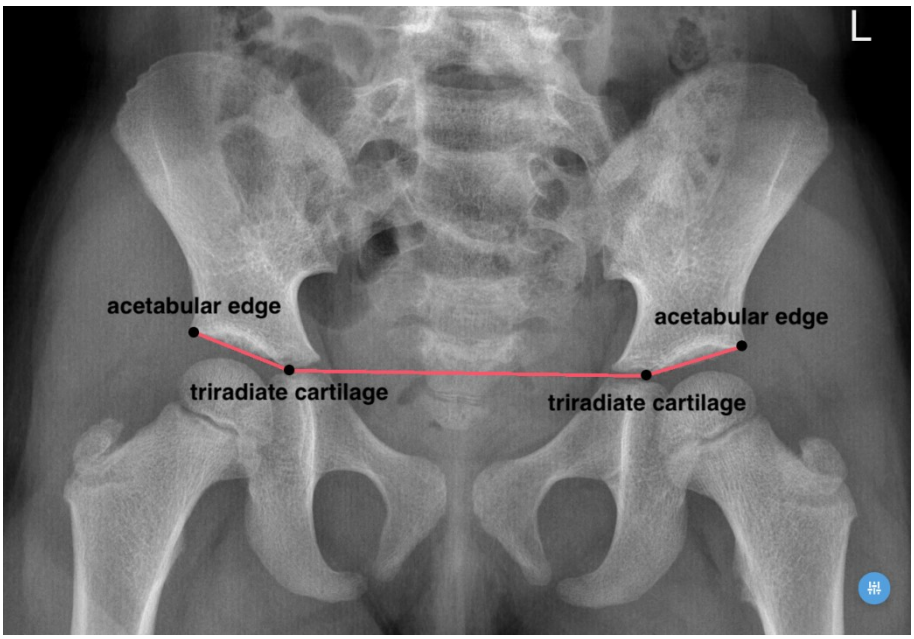

Figure 19: Identification of the AC angle in the radiograph

This X-ray image shows the necessary points to calculate the AC angle. In order to do this, the acetabular rim and the lowest point of the triradiate cartilage must be marked on one side. The same procedure should be repeated on the other side - in reverse direction.

6.4.2.2 CE angle

Before calculating the CE angle, the centre of the femoral head must be identified by using a circular template. Its midpoint is then marked on the X-ray image. Technically, the outermost point of the acetabulum is also needed for the measurement, but since this has already been identified for the AC angle (see 6.4.2.1), it is not necessary to do it again.

An imaginary orthograde line runs through the midpoint of the femoral head, while an visible line runs from the centre of the femoral head to the edge of the acetabulum (54). Then the angle between these lines is calculated, which equals the CE angle. There is no need to set a tag to represent the orthograde line. “Supervisely” calculates it based on the position of the X-ray image.

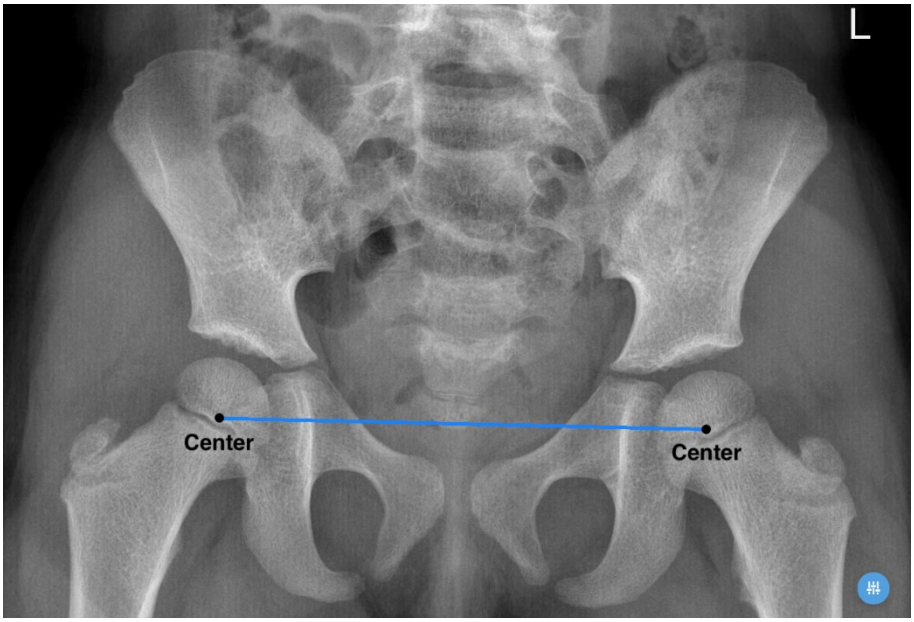

Figure 20: Identification of the CE angle in the radiograph

This figure illustrates the necessary markings for calculating the CE angle. Only the centres of both femoral heads are necessary, as the acetabular rim has already been marked for the CE angle. The centre of the femoral head is identified with the help of a circular template.

6.4.2.3 Reimer's migration index

In order to calculate the migration index according to Reimer, two more points have to be marked on the X-ray image. The first one is located at the lateral edge of the femoral head, while the second one is positioned at the medial edge of the femoral head. One again, the point in the outermost edge of the acetabulum is needed. Since this has already been set for calculating of the AC angle, it is not necessary to mark it again.

For the measurement of the migration index, three vertical lines need to be placed in the following points: the first runs through the medial border of the femoral head, the second runs through the lateral border of the femoral head and the third runs through the acetabular rim. Then the distance of the femoral head lateral to the acetabular roof (A) and the distance medial to the femoral head (B) are measured (45).

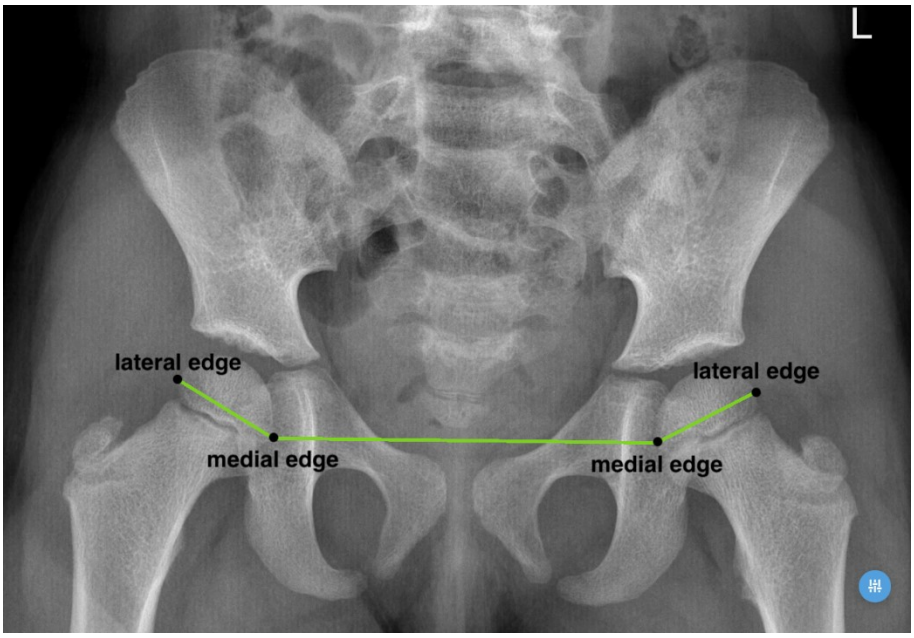

Figure 21: Identification of the MI in the radiograph

This radiograph shows which markings are required to calculate Reimer's migration index. It is necessary to mark the outermost and innermost point of the femoral head on one side. The same should be done on the other side, going from medial to lateral.

The following formula describes the calculation of the MI. A detailed explanation of how the formula is composed is described in chapter 4.45.3.

$$MI = \frac{A}{B} * 100\% \tag{45}$$

6.5 Data protection

The patient's medical history, including detailed medical reports and electronically stored data, was accessed via authorized computers on the hospital premises. This access was provided by the hospital-program "MEDOCS". First, authentication with personal access data (username and password) took place within the KAGES network. Afterwards, an additional authorisation was carried out to ensure explicit access to the confidential person-related data. In addition, every access to personal data within this system is logged and randomly controlled by data protection officials. This method helps to identify unauthorised access to confidential data within the hospital network.

Moreover, all x-rays were pseudonymised. Only the author and authorized personal were able link the pseudonym with the original data to obtain more precise information about the patient. Consequently, only the author and authorized personal had access to the original data. The patient data was stored locally and password protected.

6.6 Ethics

This study was reviewed and approved by the Ethics Committee of the Medical University of Graz on March 4, 2020 (ethics committee number 32-116 ex 19/20).

6.7 Statistical Evaluation

The following statistical analysis is a descriptive exploratory data analysis. To measure the data distribution, the following parameters are used for evaluation:

Location parameters:

- Mean
- Median
- Mode

Statistical dispersion

- Range
- Variance
- Standard deviation
- Interquartile range

7 Results

This chapter is divided into three main parts: the description of the patient collective, how the parameters change over time, and the comparison of these parameters with the reference values

7.1 Description of the patient collective

A total of 1774 X-ray images were used for evaluation. These were available from 1729 patients. Only one X-ray image was used from a total of 1678 persons, 2 images were used from a total of 48 patients, and 3 images were used from a total of 3 patients.

7.1.1 Age

The mean age of the total collective (n=1774) was 9,22 years at the time of X-ray imaging, ranging from 0,53 to 17,98 years.

Male patients were on average 9,28 years old when the radiograph was taken. The youngest male was 0,96 years and the oldest was 17,98 years old, with a Range of 17,02 years. For boys, the First Quartile was 5,46 years and the Third Quartile was 13,22 years. The Interquartile Range was 7,76. In this patient population, the median divides the data set into two equal parts at the value 9,40.

Among the female patients, the average age the x-ray was taken was 9,11 years. The youngest female was 0,53 years old and the oldest 17,95 years old. The Range of this group was 17,42 years. For this group of patients, the First Quartile was 4,63 years and the Third Quartile was 13,75 years, with an Interquartile Range of 9,12. The median age of the girls was 9,11 years.

These results are shown in the following boxplot diagram:

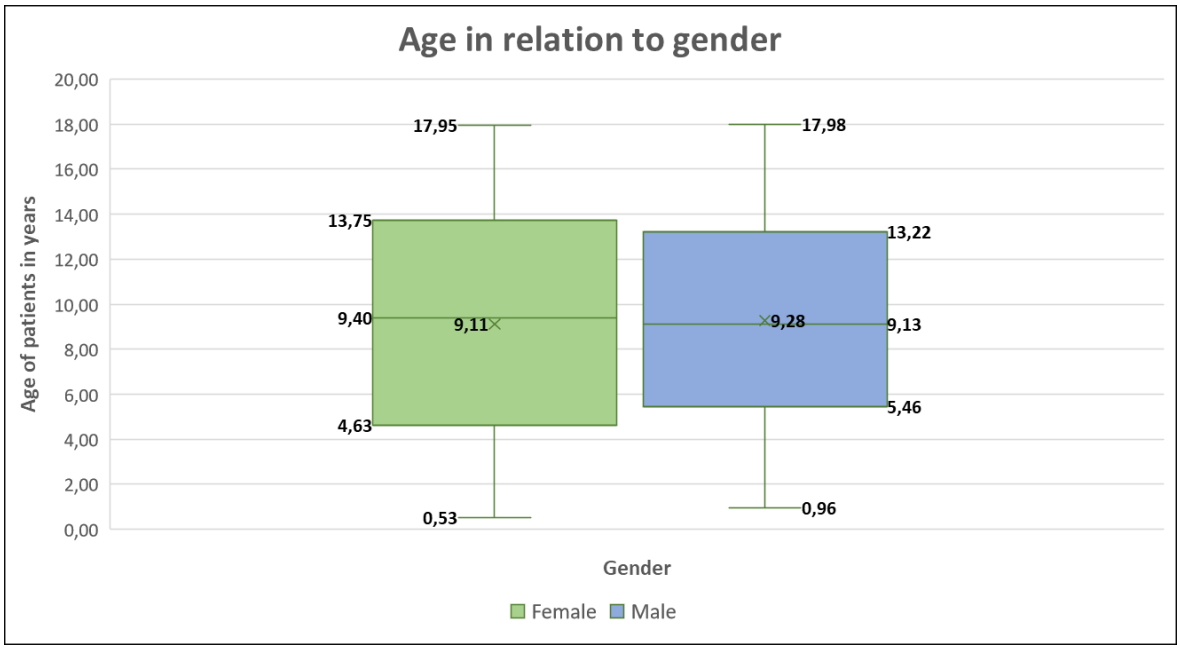

Figure 22: Age in relation to gender

This boxplot shows the distribution of the age categorized by gender. The total number of female patients was n = 666 and the total number of male patients was n = 1108. These following values are shown in the graph: Mean, Median, First Quartile, Third Quartile, Minimum and Maximum.

This graph shows the frequency distribution of girls, boys and both sexes with a range from 0 to 17 years. In the age groups from "2" to "17" there are consistently more male participants than female. There are more females than males in the age group "1", while there are slightly more females than males in the age group "0". The lowest number of participants (n=8) was in age group “0”, while the highest number of participants (n=131) was found in age group “14”.

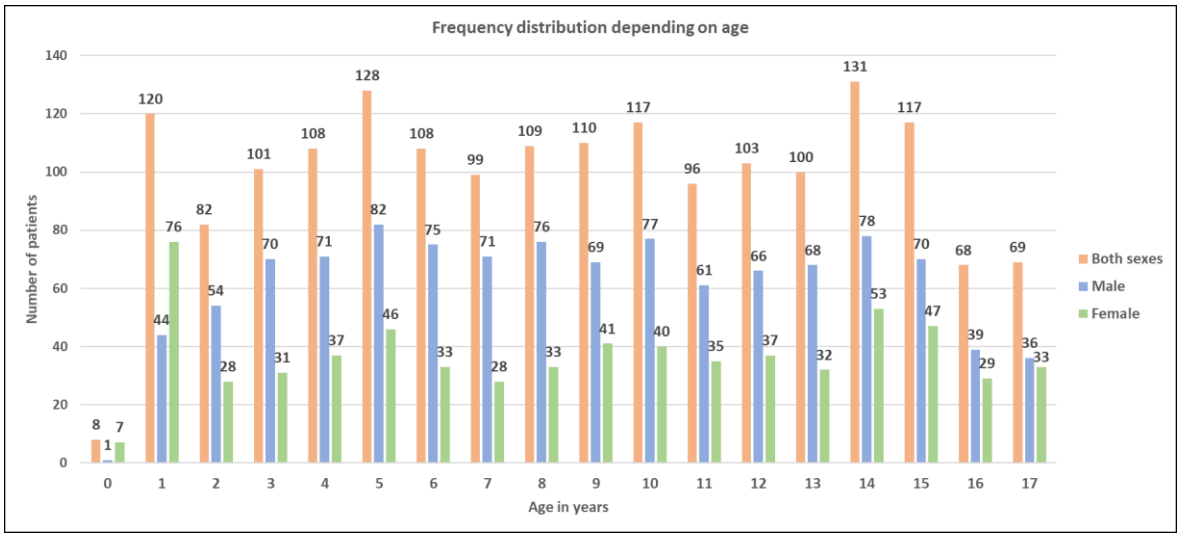

Figure 23: Frequency distribution depending on age

This graph shows the distribution of frequencies. The orange bars represent the entire patient population, the blue bars the male population and the green bars the female population.

7.1.2 Sex

The gender distribution of the included patients was random. There remained 1774 radiographs for further evaluation, of which 666 could be assigned to female and 1108 to male patients.

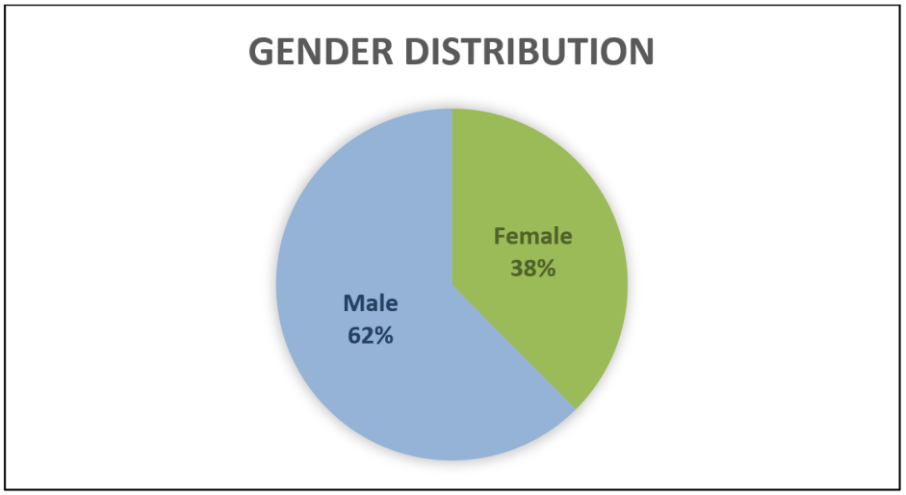

Figure 24: Gender Distribution

This graph shows the gender distribution of all data. 62% of radiographs belonged to male (n=1108) and 38% to female (n=666) patients.

7.2 Hip-specific parameters over time

The following diagrams show the size of the hip-specific parameters in relation to the patient's age. For representation of the data, multiple-line graphs are used. The x-axis reflects the age in years, while the y-axis represents the size of the hip-specific parameter. The green line represents the course of female patients, the blue line the course of male patients and the red line the course of both sexes.

7.2.1 AC angle

The following diagram shows the size of the AC angle in relation to the patient's age. While the curve of the female patients and that of both sexes start at age "0" with a starting point of approximately 23,5°, the curve representing the male starts at age "1" with a starting point of approximately 21,7°. From there, the curve declines consistently in all 3 patient groups, before leveling off slightly towards the end. The curve of the female patients ends at an age of 12 years with a value of approximately 9,2°. For the male patients, the curve ends at the age of 15 years with a value of approximately 11,2°. Since the "female" line ends at the age of 12 years, the "both sexes" line corresponds to the line of the male patients starting at the age of 12 years.

This graph shows the physiological course of the AC angle, which declines with increasing age. By comparing the graph with Table 4, it is verified that the angle-sizes can be defined as "normal" at any age and do not fall into the category of "pathological" (49).

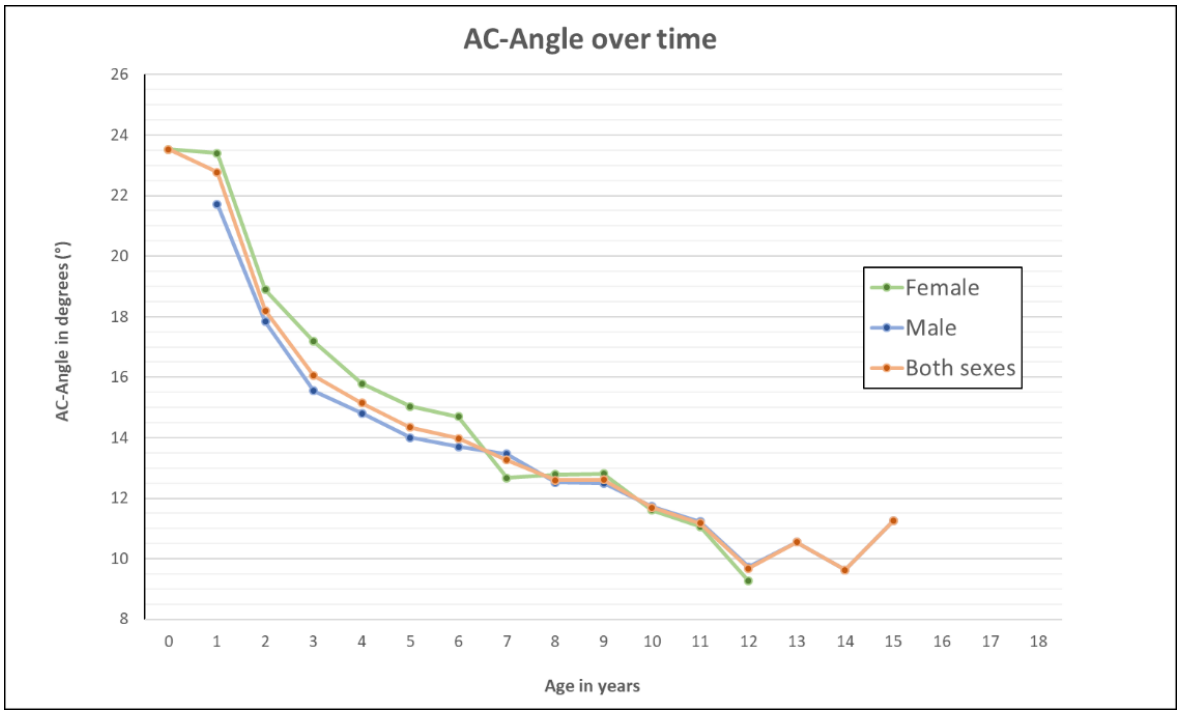

Figure 25: AC angle over time

This diagram illustrates the development of the AC angle with increasing age of the patient. It shows the development of the AC angle in females, males and both sexes.

By comparing the above graph with the existing data below, one can see the similarity in the development of the AC angle. After birth, there is a greater decrease in the angle, which continues to flatten as it progresses. Although the graph below shows the development of the AC angle only up to the age of 5, it can be assumed that there will be a comparable development in the following years due to the similarity of both curves.

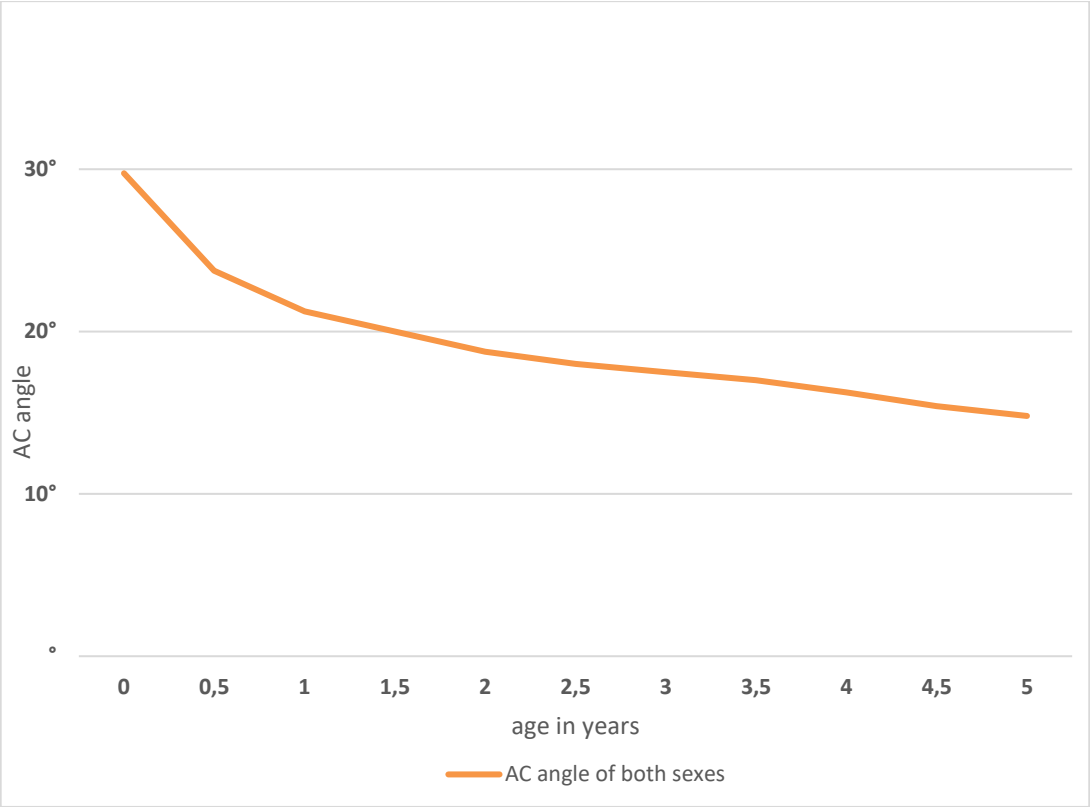

Figure 26: Graphical representation of the AC angle of the already existing data

In this diagram, boys and girls are not shown separately. There is a noticeable drop in the AC angle after birth. The curve is steeper at first, but then gradually flattens out. Adopted with modification by (37).

7.2.2 CE angle

The illustrated graph gives information about the development of the CE angle depending on patient's age. For female patients, the curve begins at an age of “0”, while the males have their starting point at an age of “1”. At the beginning there is a short drop in the curves of female patients, but after that the groups increase almost linearly. The curves stop at an age of "18" and while the female patients reach an AC angle of about 35°, the male patients reach about 38° and the value for both sexes (the mean between these two) is 36,5°.

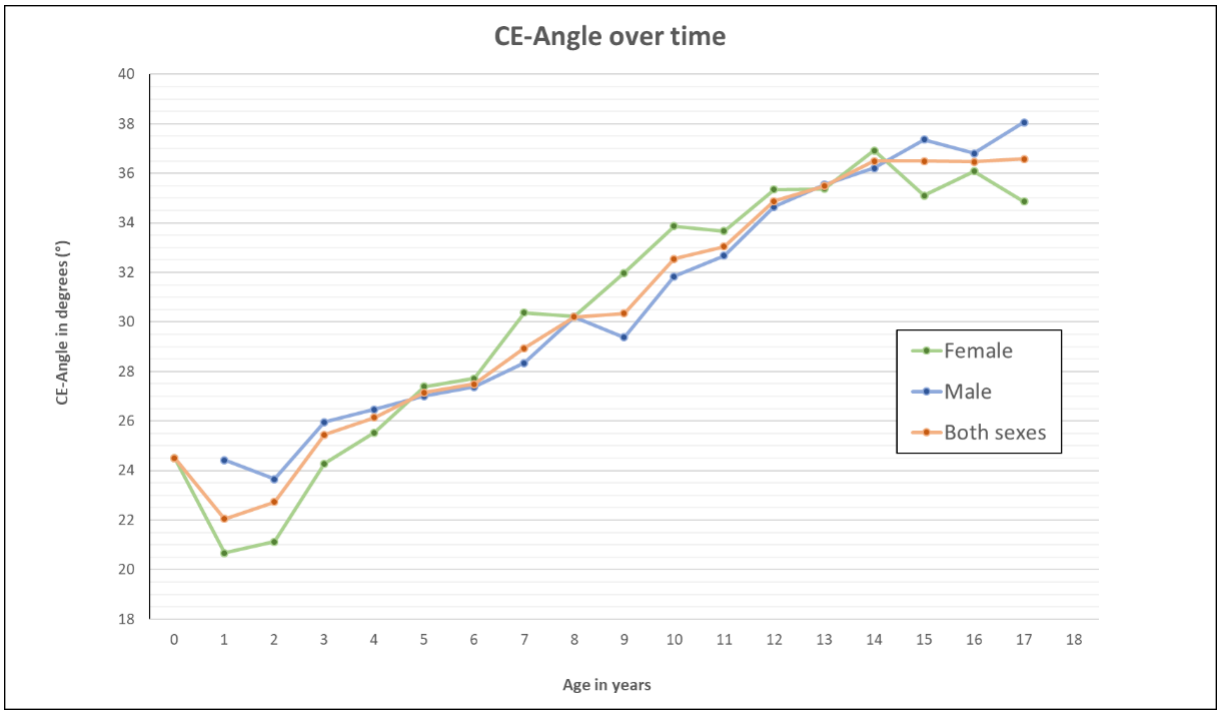

Figure 27: CE angle over time

This graph gives information about the CE angle in relation to age. It shows data of females, males and both sexes and there is an upward trend in the size of the CE angle over the 18 years.

By comparing the above graph with that of Brückl a definite similarity in the shape of the curve can be seen. Aside from that, Tönnis' results (see Table 3) confirm that the measured AC angles are considered physiological and not pathological. The graph below first starts at the age of 5 and ends at the age of 20. Since this thesis only considered participants under the age of 18, older individuals are not shown in the graph above.

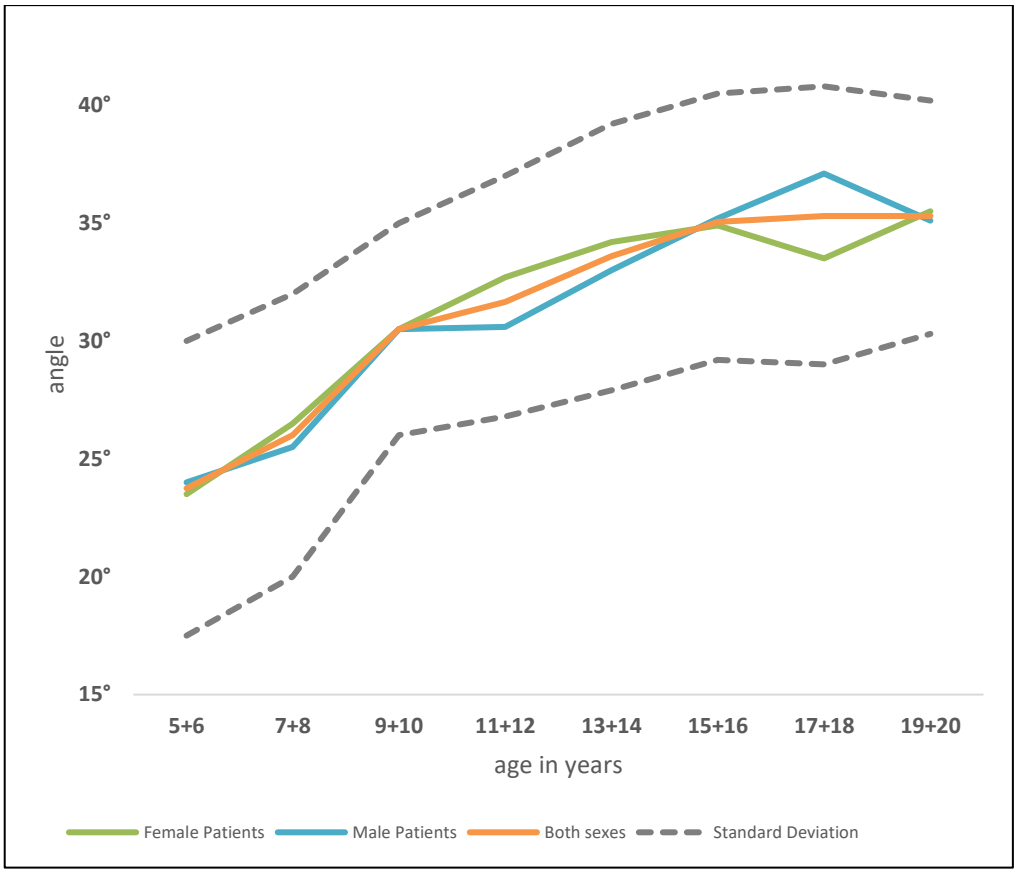

Figure 28: Graphical representation of the CE angle of the already existing data

This chart shows the development of the CE angle between the ages of 5 and 20. The female and male values are shown separately. After the age of 5, there is an inclination of the angle, which increases more slowly the older the patients get. Adopted with modification by (48).

7.2.3 Reimer's migration index

The following diagram represents the size of Reimer's migration index dependent on patients age. The curve of female patients starts at a baseline of "3%" at age "0", while the curve of the male patients starts at approximately "3,5%" at age "1".

As the graph shows, the migration index increases as the patients get older. Compared to the two upper diagrams (Figure 25 and Figure 27), a larger scattering of values can be observed, as there are more sudden drops and jumps than in the other diagrams. The curve ends at an age of "18" for females and males. The

females reach a value of approximately 11,4%, the males of approximately 8,9% and the value of both sexes compared is approximately 10%. It should also be noted that all values between 10% and 30% are classified as "mildly subluxated".

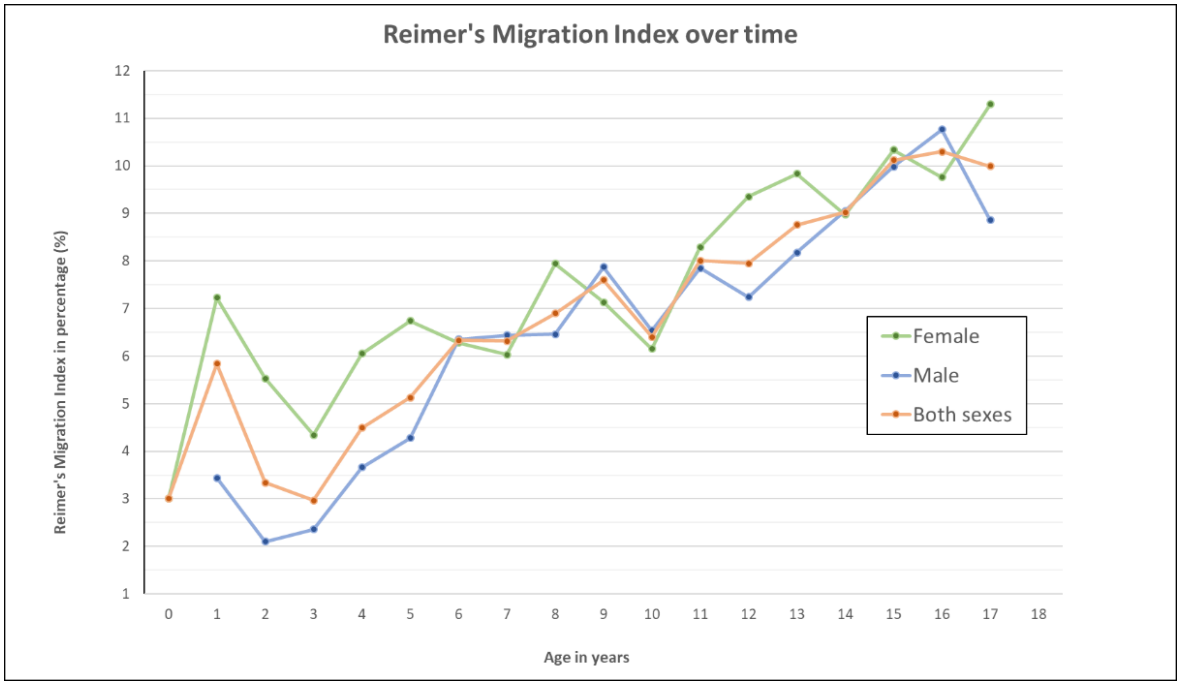

Figure 29: Reimer’s migration index over time

This graph illustrates the progression of the migration index in relation to patient age. Data of girls, boys and both sexes compared are analysed.

7.3 Direct comparison of data

In the following chapter, the data collected for the diploma thesis are compared with those from the literature.

7.3.1 Comparison of the AC angle

The following table is a representation of the original data from the study “"Eine Abgrenzung normaler und pathologischer Hüftpfannendachwinkel zur Diagnose der Hüftdysplasie" written by D. Tönnis and D. Brunken. It shows the mean values of the AC angle at an age of 3 months up to 14 years and demonstrates that the AC angle should decrease with age.

The table also shows the classification for AC angles that are within and over the normal range. This classification runs from grade 1 (=normal) to grade 4 (extremely pathological) (49).

Age (years/months)	Mean value	Grade I (normal)	Grade II (mildly pathological)	Grade III (severely pathological)	Grade IV (extremely pathological)
0/3 + 0/4	25	<30	≥30 - <35	≥35 - <40	≥40
0/5 – 2/0	20	<25	≥25 - <30	≥30 - <35	≥35
2 – 3	18	<23	≥23 - <28	≥28 - <33	≥33
3 – 7	15	<20	≥20 - <25	≥25 - <30	≥30
7 - 14	10	<15	≥15 - <20	≥20 - <25	≥25

Table 6: Illustration of the AC angles according to Tönnis and Brunken

This table shows the results of Tönnis and Brunken's study. The calculated mean values represent the AC angles of 5 different age groups. It also illustrates up to which point the AC angle is considered normal and from which point it is considered mildly, severely or extremely pathological. Adopted with modification by (49).

The following table shows the data collected as part of this thesis. To enable an accurate comparison, only age groups between 0 and 14 years were considered here, same as in table 6. Patients between the ages of 3 and 4 months were not included in the data analysis. For this reason, no AC angle is described for this group of patients. One reason why pelvic X-ray images are rarely indicated in this age group is that accidents are less likely to occur while baby's are still crawling. Therefore, radiography to evaluate fractures is not necessary. In addition, diseases that are clarified by means of X-ray diagnostics, such as coxitis fugax or ECF, usually occur at a later age. Diseases of the hip joint that are diagnosed using X-ray diagnostics, such as coxitis fugax or ECF usually occur at a later age.

The table shows that all AC angles used in this diploma thesis can be classified as "normal" as they are within the normal range specific to their age group (see Table 6). Based on these results, it can be assumed that the existing reference values of the AC angle for the age group between 4 months and 14 years are still valid.

Age **(years/months)**	AC angle (°) **(mean value)**	Number **(n)**
0/3 + 0/4	/	0
0/4 – 2/0	22,82	121
2 – 3	18,21	78
3 – 7	14,85	438
7 – 14	11,96	567

Table 7: AC angles calculated as part of the diploma thesis

This table shows the calculated mean values of the AC angles. Categorisation of the age groups corresponds to the table of Tönnis and Brunken. As there are no participants in the age group between 3 and 4 months, no AC angle could be calculated.

7.3.2 Comparison of the CE angle

CE angle according to Scoles

In his study, Scoles only considered children who were between 3 and 24 months old. Since only 8 children fell into this age group it would not be reasonable to statistically analyse this data and present it here.

CE angle according to Brückl

Brückl's study included patients from 5 to 20 years of age, where he compared the CE angle of male and female patients. He presented the calculated angles using the mean values and the standard deviation (see Table 8). The CE angle should usually be at least 15° in children and increases with age (48).

Age (years)	Girls	Number	Boys	Number
5 + 6	23,5 ± 6,0	106	24,0 ± 6,6	80
7 + 8	26,5 ± 6,2	76	25,5 ± 6,0	64
9 + 10	30,5 ± 4,7	128	30,5 ± 4,6	60
11 + 12	32,7 ± 5,4	92	30,6 ± 4,7	46
13 + 14	34,2 ± 4,8	68	33,0 ± 6,3	66
15 + 16	34,9 ± 6,1	77	35,2 ± 4,9	43
17 + 18	33,5 ± 5,4	56	37,1 ± 6,0	38
19 + 20	35,5 ± 5,3	56	35,1 ± 4,3	54

Table 8: Illustration of the CE angles according to Brückl

This table shows the CE angles ascertained by Brückl. His data is presented as mean values to which he has also added the standard deviation. Brückl analysed the CE angles for 8 different age groups, with patient ages from 5 to 20 years. He published the CE angles separated by sex. Adopted with modification by (48).

The next table shows the results of the CE angle that were gathered in the process of this thesis. While Brückl's study included patients between the ages of 5 and 20, the maximum age for this diploma thesis is defined as 17,99 years. For this reason, patients aged 18 to 20 years are not included in the following table. The age groups on the following table are arranged on the basis of Brückl's categorisation and there is also a gender-based classification. All mean values shown here extend beyond an angle of 15° and are thereby within the official norm, they can be considered physiological. An increase in the size of the angles with rising age can be observed.

Age (years)	Female		Male	
	CE angle (°) ± standard deviation	Number (n)	CE angle (°) ± standard deviation	Number (n)
5 + 6	27,54 ± 5,08	77	27,19 ± 4,98	158
7 + 8	30,30 ± 4,83	60	29,28 ± 4,60	143
9 + 10	32,90 ± 4,54	84	30,65 ± 4,53	149
11 + 12	34,49 ± 4,84	69	33,71 ± 5,21	128
13 + 14	36,30 ± 5,03	86	35,91 ± 5,53	144
15 + 16	35,50 ± 5,30	78	37,19 ± 4,75	110
17 – ≤ 18	34,86 ± 4,34	33	38,06 ± 5,66	38

Table 9: CE angles calculated as part of the diploma thesis

This table represents the CE angles that were calculated for this diploma thesis. The structure and organisation of the table correlates with Brückl's. Since no CE angles of patients older than 18 years were collected, this table only consists of 7 age groups

CE angle according to Tönnis

In 1984, Tönnis evaluated the CE angles of patients between the ages of 0 and 50 years. Therefore, he divided the age groups into three fractions: 0 to 8 years, 8 to 18 years and 18 to 50 years. He presented the age-dependent CE angles using the mean values of his measurements without a gender-specific differentiation. The table also describes those values that are within and above the defined normal range. This classification goes from grade 1 (=normal) to grade 4 (extremely pathological) (49).

Age (years)	Mean value	Grade I (normal)	Grade II (mildly pathological)	Grade III (severely pathological)	Grade IV (extremely pathological)
≥0 - ≤8	25	≥20	≥15 - <20	≥0 - <15	<0
≥8 - ≤18	32	≥25	≥20 - <25	≥5 - <20	<5
≥18 - 50	35	≥30	≥20 - <30	≥5 - <20	<5

Table 10: Illustration of the CE angles according to Tönnis

This table summarises the results of Tönnis' 1984 study. The CE angles are presented as normal values in 3 different age groups. Like in Table 6, Tönnis defines at which point an angle is considered mildly, severely or extremely pathological. Adopted with modification by (49).

As already indicated, this diploma thesis deals exclusively with patients aged 0 and 18 years. For this reason, the following table is structured similarly to that of Tönnis, but the age group from 18 to 50 years was excluded. The values in this table are very similar to those of Tönnis and all lie within the defined physiological range categorised as "normal".

Age (years)	CE angle (°)	Number (n)
≥ 0- ≤ 8	25,77	751
> 8 - 18	34,13	1002

Table 11: CE angles calculated as part of the diploma thesis

This table is a representation of the CE angles that were calculated for the diploma thesis. Age group classification with the one of Tönnis, but does not include patients older than 18 years.

7.3.3 Comparison of Reimer's migration index

As mentioned in Reimer's migration index5.3, Reimer's migration index was not included in Exner's book "Normalwerte in Wachstum und Entwicklung" (3). Yet it is an important parameter of the child's hip and should therefore be mentioned. Comparative values for this were taken from the article "Hip surveillance in Tasmanian children with cerebral palsy" by A. Connelly and P. Flett instead of Exner's book. This article provided information when a hip is considered normal, subluxated or dislocated (51).

Migration percentage (%)	Definition and progression
0 – 10	Normal
10 – 30	Mild subluxation
30 – 60	Moderate subluxation
60 – 90	Severe subluxation
> 90	Dislocated

Table 12: Illustration of Reimer's MI according to Connelly and Flett

This table shows the value of the migration index (in percent), to determine when a hip joint is considered normal and when it is considered subluxated or dislocated. Adopted according to (51).

The following table shows the results of the migration index collected for this thesis. The left column shows the age of the patients, ranging from 0 to 17,99 years. The migration index was calculated for each year of life. In the two middle columns, the migration index is presented both as a decimal number and as a percentage, while the right column provides information on the number of patients.

Age (years)	Migration index: Relative frequency	Migration index: Relative frequency in percent (%)	Number (n)
0 – 0,99	0,030	3,0	6
1 – 1,99	0,058	5,8	117
2 – 2,99	0,033	3,3	80
3 – 3,99	0,030	3,0	101
4 – 4,99	0,045	4,5	112
5 – 5,99	0,051	5,1	124
6 – 6,99	0,063	6,3	111
7 – 7,99	0,063	6,3	100
8 – 8,99	0,069	6,9	103
9 – 9,99	0,076	7,6	115
10 – 10,99	0,064	6,4	118
11 – 11,99	0,080	8,0	96
12 – 12,99	0,080	8,0	101
13 – 13,99	0,088	8,8	100
14 – 14,99	0,090	9,0	130
15 – 15,99	0,101	10,1	121
16 – 16,99	0,103	10,3	67
17 – 17,99	0,099	9,9	71

Table 13: Reimer's MI calculated as part of the diploma thesis

This table shows the development of the migration index with increasing age. The migration index is thereby presented as a decimal number and as a percentage.

This graph shows that the migration index increases with age. In all but two age groups, the values are within the norm (0-10%) for a "normal" hip joint. In the "15-15,99" and "16-16,99" age groups, the 10% limit is exceeded by a minimum of 0,1% and 0,3%, respectively. Since it can be assumed that measurement errors occurred in the calculation of the migration index even when working exactly, this marginal increase in the values has no real significance.

8 Discussion

The aim of this study was to evaluate whether the current radiological parameters to evaluate the growing hip are still up-to-date, as these were derived from outdated studies with a small number of participants. Pelvic overview radiographs of 3786 patients aged 0 to 18 years were available for data analysis. Because only radiographs of healthy children's hips were included in the analysis, a total of 1774 suitable pelvic radiographs remained for further evaluation after closer examination. Among the radiographs 666 belonged to girls with an average age of 9,11 years and 1108 belonged to boys with an average age of 9,28 years.

AC angle

The calculation and evaluation of the AC angle confirmed that the measured mean values for all age groups are within the norm defined by Tönnis and Brunken (see Table 6). In other words, they do not exceed the maximal value of the AC angle and are therefore considered physiological. This indicates that the femoral head is adequately covered by the acetabulum at all ages present. No data are available for children older than 15 years, which is mainly explained by the fact that the triradiate cartilage ossifies at the age of 15 years, often even earlier. As a result, it is no longer possible to draw the Hilgenreiner’s line, which is an essential element for calculating the AC angle. Figure 25 shows the physiological progression of the AC angle: with increasing age, the angle becomes progressively smaller.

CE angle

The comparison of the CE-Angels was carried out exclusively with the data from the study by Brückl and Tönnis. The results of Scoles' study could not be considered because he only examined children aged 3 to 24 months. Only 8 children matched this age group and evaluation would not have been valid with a patient population of this size.

To be classified physiological, the CE angle must be at least 15° and should increase with age (48). All mean values of the CE angle measured for this thesis fulfilled this condition, as they were greater than 15°. In his study, Brückl analysed

the CE angles of both sexes separately and presented them as mean values and standard deviations. For a better comparability, the values of the CE angles in this thesis were also presented as mean values including standard deviations. Comparing the calculated values (Table 9) with those of Brückl's table (Table 8), the difference between the angles in the age groups from 5 to 8 years is about 4°. In the age group between 9 and 14 years, the measured CE angles are approximately 2° larger than those of Brückl. Reasons for this could be the better X-ray resolution compared to that time, and the more accurate measurement with the method used in this age group. In the age group between 15 and 18 years, the measured CE angles are merely 1° larger. Despite these minor differences, all measured values are within the physiological norm. In each of these two tables, the physiological changes in the CE angle over the time can be observed as the angles increase with the patient's age. Tönnis' study (see Table 10) also confirms that the values measured for the CE angle (see Table 11) can be considered physiological, since the angles are larger than the lower limit of the CE angle defined by him. The comparison of the calculated values with the available data shows that there is sufficient coverage of the femur by the acetabular roof in the corresponding patient groups.

Reimer's migration index

The migration index is defined as the percentage of the ossified femoral head outside the lateral margin of the ossified acetabulum. It shows the decentration of the femoral head to determine the extent of lateralization (55). Exner's book "Normalwerte in Wachstum und Entwicklung" (3) does not elaborate on the migration index, so data from the study "Hip surveillance in Tasmanian children with cerebral palsy" (51) were used for this thesis.

Table 12 shows how high the migration index must be to consider a hip joint as "normal", "mildly subluxated", "moderately subluxated", "severely subluxated" or "dislocated". Table 13 shows the measured migration indexes for the diploma thesis, with values calculated for each year of life. In the age groups "15-15,99" and "16-16.99", the migration index was minimally (up to 0,3%) above the 10% threshold. Exceeding the cut-off value should not be immediately interpreted as pathological,

since errors can be made even with accurate measurement. To clarify these values more precisely, further studies of the migration index in this age group with a higher number of patients would be necessary. In the remaining age groups, the migration index is physiological, as the values are smaller than 10%. The natural progression of the migration index, which becomes larger with increasing age, can also be observed.

Today's relevance of the results

Considering the fact that the studies Exner used in his book are several decades old, it is surprising that there has not been a significant change in the hip-specific parameters, despite the shift in children's living conditions today. One of the reasons why changes in the pediatric hip joint could be expected is the increasing obesity in childhood. As the study "Global Evolution of Obesity Research in Children and Youths: Setting Priorities for Interventions and Policies" has shown, childhood obesity has become a major global problem (56). A WHO study says that "the worldwide prevalence of obesity nearly tripled between 1975 and 2016" and that "the prevalence of overweight and obesity among children and adolescents aged 5-19 has risen dramatically from just 4% in 1975 to just over 18% in 2016" (1). It would have been reasonable that increasing obesity would have an effect on the musculoskeletal system, but as the study "The Impact of Fat and Obesity on Bone Microarchitecture and Strength in Children" by Joshua N. Farr and Paul Dimitri states, "The effects of weight, on physical development are more minimal than expected. […] Nonetheless, a linear relationship between increasing adiposity and skeletal development seems unlikely" (2).

With the increased obesity of children today also comes the premature onset of puberty. The study "Early Maturity as the New Normal: A Century-long Study of Bone Age" by Melanie Boeyer shows that in children born in the last 20 years, the growth plates closed significantly earlier than in previous generations. In boys, the time of completed bone growth advanced by an average of seven months, and in girls by almost ten months (57). Taking a closer look at the ossification of the Y-shaped cartilage, there are no radiographs available for children older than 15 years where the growth plate has not yet closed. This is mainly because the triradiate

cartilage usually ossifies at the age of 15, often even earlier. In this study, the question of whether there is a connection with premature onset of puberty was not specifically evaluated and would have to be analyzed separately in another study.

Limitations:

A limitation of this thesis is that, despite the overall large number of patients, there were occasionally only a few participants in individual age groups. Statistical comparisons with a small number of subjects have less validity than those with a large number. Large study populations minimize the influence of random fluctuations.

Another limitation of this thesis was the unbalanced gender distribution with a predominance of male patients. Overall, there were noticeably more pelvic X-rays available from male patients than from female patients. This is likely due to boys being more willing to take risks in everyday life, such as playing games or doing sports. The availability of X-ray images due to trauma would explain the increased number of X-ray images in boys.

Marking the points on the pelvic radiographs was another limitation and occasionally problematic, as the outermost margin of the acetabulum and the triradiate cartilage could not always be clearly identified.

8.1 Conclusion

The data collected for this thesis demonstrate that the studies on hip-specific angles (AC angle and CE angle) presented in Exner's book “Normalwerte in Wachstum und Entwicklung” are still relevant and should continue to be used for evaluation of the pediatric hip. Also, the existing data on Reimer's migration index are still valid and should be used to determine the decentralization of the femoral head.

9 References

1. WHO. Obesity and overweight [Internet]. [cited 2021 Nov 9]. Available from: https://www.who.int/news-room/fact-sheets/detail/obesity-and-overweight

2. Farr JN, Dimitri P. The Impact of Fat and Obesity on Bone Microarchitecture and Strength in Children. Calcif Tissue Int. 2017 May 1;100(5):500–13.

3. Exner U, editor. Normalwerte in Wachstum und Entwicklung [Internet]. 2nd ed. Stuttgart: Georg Thieme Verlag; 2003 [cited 2019 Nov 11]. 90–97 p. Available from: http://www.thieme-connect.de/products/ebooks/book/10.1055/b-002-15438

4. Waschke J, Böckers TM, Paulsen F, Arnold WH, Bechmann IJ, Böckers A, et al. Anatomie das Lehrbuch: Sobotta. 2019. 216 ff.

5. Waldeyer A, Anderhuber F, editors. Waldeyer - Anatomie des Menschen: Lehrbuch und Atlas in einem Band. 19., vollst. überarb. und aktualisierte Aufl. Berlin: de Gruyter; 2012. 602 p.

6. Tönnis D. Die angeborene Hüftdysplasie und Hüftluxation im Kindes- und Erwachsenenalter: Grundlagen, Diagnostik, konservative und operative Behandlung: mit 346 Abbildungen in 814 Einzeldarstellungen und 49 Tabellen. Berlin New York Tokyo: Springer-Verlag; 1984. 129–34 p.

7. Waldeyer A, Anderhuber F, editors. Waldeyer - Anatomie des Menschen: Lehrbuch und Atlas in einem Band. 19., vollst. überarb. und aktualisierte Aufl. Berlin: de Gruyter; 2012. 342 p.

8. Aumüller G, Aust G, Conrad A, Engele J, Kirsch J, Maio G, et al. Duale Reihe Anatomie [Internet]. 5th ed. Stuttgart: Georg Thieme Verlag; 2020 [cited 2021 Jul 12]. Available from: https://eref.thieme.de/10.1055/b-007-170976

9. Dauber W, Feneis H, Spitzer G. Feneis' Bild-Lexikon der Anatomie: über 8.000 anatomische Fachbegriffe - über 800 Abbildungen ; nach der neuen offiziellen internationalen Terminologie (FCAT) ; zusätzlich mit englischem Sachverzeichnis. 9., komplett überarb. Aufl. Stuttgart: Thieme; 2005. 66 f.

10. Proximal Femur - an overview | ScienceDirect Topics [Internet]. [cited 2021 Jul 13]. Available from: https://www.sciencedirect.com/topics/medicine-and-dentistry/proximal-femur

11. Sobotta 1909 fig.137 - femur, posterior view - colour, no labels | AnatomyTOOL [Internet]. [cited 2021 Jul 13]. Available from: https://anatomytool.org/content/sobotta-1909-fig137-femur-posterior-view-colour-no-labels

12. Schünke M, Schulte E, Schumacher U, Voll M, Wesker KH. PROMETHEUS Allgemeine Anatomie und Bewegungssystem: LernAtlas der Anatomie [Internet]. 5th ed. Stuttgart: Georg Thieme Verlag; 2018 [cited 2021 Aug 29]. Available from: https://eref.thieme.de/images/l/866427_25.jpg

13. Hepp WR, Locher H, Graf R. Orthopädisches Diagnostikum. 8., überarb. und erw. Aufl. Stuttgart: Thieme; 2014. 169–75 p.

14. Waldeyer A, Anderhuber F, editors. Waldeyer - Anatomie des Menschen: Lehrbuch und Atlas in einem Band. 19., vollst. überarb. und aktualisierte Aufl. Berlin: de Gruyter; 2012. 315 ff.

15. Tschauner C, Aigner RM, Wirth C-J, editors. Becken, Hüfte: 114 Tabellen. Stuttgart: Thieme; 2004. 10 ff. (Orthopädie und orthopädische Chirurgie [: das Standardwerk für Klinik und Praxis]).

16. Schatz P. Hip Joint. In: Anatomy and Physiology [Internet]. Houston, Texas: OpenStax; (J. Gordon Betts, Kelly A. Young, James A. Wise, Eddie Johnson, Brandon Poe, Dean H. Kruse, Oksana Korol, Jody E. Johnson, Mark Womble, Peter DeSaix, editor. Anatomy and Physiology). Available from: https://openstax.org/books/anatomy-and-physiology/pages/1-introduction

17. Retchford TH, Crossley KM, Grimaldi A, Kemp JL, Cowan SM. Can local muscles augment stability in the hip? A narrative literature review. J Musculoskelet Neuronal Interact. 2013 Mar;13(1):1–12.

18. Schünke M, Schulte E, Schumacher U. Allgemeine Anatomie und Bewegungssystem. 4., überarbeitete und erweiterte Auflage. Voll M, Wesker K, editors. Stuttgart New York: Georg Thieme Verlag; 2014. 555 p. (Prometheus).

19. Ilipsoas (Iliopectineal) Bursa [Internet]. Earth's Lab. [cited 2021 Jul 13]. Available from: https://www.earthslab.com/anatomy/ilipsoas-iliopectineal-bursa/

20. Christ B, editor. Anatomie. 1: Zellen- und Gewebelehre, Entwicklungslehre, Skelett- und Muskelsystem, Atemsystem, Verdauungssystem, Harn- und Genitalsystem / [unter Mitarb. von B. Christ]. 17., durchges. Aufl. München Jena: Elsevier, Urban & Fischer; 2008. 358 ff.

21. Sobotta - Atlas der Anatomie. Band 4: Tabellen zu Muskeln, Gelenken und Nerven. 3. Auflage. München: Elsevier; 2017. 57 ff.

22. Amboss GmbH. Becken und Hüfte - Wissen für Mediziner [Internet]. [cited 2020 Nov 10]. Available from: https://www.amboss.com/de/wissen/Becken_und_H%C3%BCfte

23. Larnert P, Risto O, Hägglund G, Wagner P. Hip displacement in relation to age and gross motor function in children with cerebral palsy. J Child Orthop. 2014 Mar;8(2):129–34.

24. Breusch SJ, Clarius M, Mau H, Sabo D. Klinikleitfaden Orthopädie Unfallchirurgie [Internet]. 8th ed. 2020 [cited 2019 Nov 11]. 651 ff. Available from: https://www.sciencedirect.com/science/book/9783437224751

25. Tönnis D. Die angeborene Hüftdysplasie und Hüftluxation im Kindes- und Erwachsenenalter: Grundlagen, Diagnostik, konservative und operative Behandlung: mit 346 Abbildungen in 814 Einzeldarstellungen und 49 Tabellen. Berlin New York Tokyo: Springer-Verlag; 1984. 12ff.

26. Abteilung Medizin, Universität Freiburg. Osteogenese [Internet]. 2021 [cited 2021 Aug 23]. Available from: https://www3.unifr.ch/apps/med/elearning/de/stuetzgewebe/osteogenese/d-osteogenese.php

27. Tschauner C, Aigner RM, Wirth C-J, editors. Becken, Hüfte: 114 Tabellen. Stuttgart: 4 f.; 2004. 4 p. (Orthopädie und orthopädische Chirurgie [: das Standardwerk für Klinik und Praxis]).

28. Uhthoff HK, Jarvis J. Embryologie der menschlichen Hüfte. Orthopäde. 1997 Jan 30;26(1):2–6.

29. Exner U, editor. Normalwerte in Wachstum und Entwicklung [Internet]. 2nd ed. Stuttgart: Georg Thieme Verlag; 2003 [cited 2021 Aug 23]. 77f. Available from: http://www.thieme-connect.de/products/ebooks/book/10.1055/b-002-15438

30. Femur Bone - Anterior Markings [Internet]. GetBodySmart. 2017 [cited 2021 Aug 23]. Available from: https://www.getbodysmart.com/lower-limb-bones/femur-bone-anterior-markings

31. Ráliš Z, McKibbin B. Changes in shape of the human hip joint during its development and their relation to its stability. The Journal of Bone and Joint Surgery British volume. 1973 Nov 1;55-B(4):780–5.

32. Niethard FU, Pfeil J, Biberthaler P, Hoffmann M, Gusta M, Gusta P, et al. Orthopädie und Unfallchirurgie: 1135 Abbildungen. 8., unveränderte Auflage. Stuttgart: Thieme; 2017. 522 ff. (Duale Reihe).

33. Mau H, Breusch S, Weber M-A, Beyer T, Ackermann O, Schneidmüller D. Bildgebende Diagnostik in der Orthopädie. In: Breusch S, Clarius M, Mau H, Sabo D, Abel R, Ackermann O, et al., editors. Klinikleitfaden Orthopädie Unfallchirurgie (Neunte Ausgabe) [Internet]. Munich: Urban & Fischer; 2019 [cited 2021 Aug 23]. p. 81–123. (Klinikleitfaden). Available from: https://www.sciencedirect.com/science/article/pii/B9783437224751000044

34. Narayanan U, Mulpuri K, Sankar WN, Clarke NMP, Hosalkar H, Price CT. Reliability of a New Radiographic Classification for Developmental Dysplasia of the Hip. Journal of Pediatric Orthopaedics. 2015 Jul;35(5):478–84.

35. Wiberg G. Studies on Dysplastic Acetabula and Congenital Subluxation of the Hip Joint: With Special Reference to the Complication of Osteoarthritis [Internet]. Norstedt; 1939. 7–38 p. Available from: https://books.google.at/books?id=T1PUoAEACAAJ

36. Waldt S, Woertler K, editors. Measurements and Classifications in Musculoskeletal Radiology [Internet]. Stuttgart: Georg Thieme Verlag; 2014 [cited 2020 Nov 10]. Available from: https://radiologykey.com/hipii/#c002_f028

37. Hefti F. Kinderorthopädie in der Praxis [Internet]. Berlin, Heidelberg: Springer Berlin Heidelberg; 2014 [cited 2019 Nov 9]. 219 p. Available from: http://link.springer.com/10.1007/978-3-642-44995-6

38. Assoc Prof Gaillard F. Hilgenreiner's line [Internet]. Radiopaedia. [cited 2020 Nov 10]. Available from: https://radiopaedia.org/cases/hilgenreiner-s-line

39. Pschyrembel Online | Azetabulumwinkel [Internet]. [cited 2021 Jul 14]. Available from: https://www.pschyrembel.de/Azetabulumwinkel/K01CD

40. Baumgart K, Mellerowicz H. Hüftdysplasie. Orthopädie und Unfallchirurgie up2date. 2013 Mar 6;8(01):579ff.

41. Windhagen H, Thorey F, Kronewid H, Pressel T, Herold D, Stukenborg-Colsman C. The effect of functional splinting on mild dysplastic hips after walking onset. BMC Pediatr. 2005 Dec;5(1):17.

42. Assoc Prof Gaillard F. Acetabular angle [Internet]. Radiopaedia. [cited 2020 Nov 10]. Available from: https://radiopaedia.org/cases/acetabular-angle-diagram?lang=us

43. Ruchholtz S, Wirtz DC. Orthopädie und Unfallchirurgie essentials Intensivkurs zur Weiterbildung. 2019. 259 p.

44. Strobl W. Neuromuskuläre Erkrankungen. In: Tschauner C, editor. Orthopädie und Orthopädische Chirurgie - Becken, Hüfte [Internet]. Stuttgart: Georg Thieme Verlag; 2004 [cited 2019 Nov 9]. p. 260. Available from: https://eref.thieme.de/10.1055/b-002-6231

45. Hefti F, Brunner R, Hasler C, Jundt G, Krieg A, Freuler FK. Kinderorthopädie in der Praxis. 3., vollst. überarb. Aufl. Berlin: Springer; 2015. 283 p.

46. Neirynck J, Proost R, Van Campenhout A. The migration percentage measured on EOS® standing full-leg radiographs: equivalent and advantageous in ambulant children with cerebral palsy. BMC Musculoskelet Disord. 2019 Dec;20(1):366.

47. Scoles PV, Boyd A, Jones PK. Roentgenographic parameters of the normal infant hip. J Pediatr Orthop. 1987 Dec;7(6):656–63.

48. Brückl R, Hepp WR, Tönnis D. Eine Abgrenzung normaler und dysplastischer jugendlicher Hüftgelenke durch den Hüftwert. Archiv für orthopädische und Unfall-Chirurgie, mit besonderer Berücksichtigung der Frakturenlehre und der orthopädisch-chirurgischen Technik. 1972 Mar 1;74(1):13–32.

49. Tönnis D. Die angeborene Hüftdysplasie und Hüftluxation im Kindes- und Erwachsenenalter: Grundlagen, Diagnostik, konservative und operative Behandlung: mit 346 Abbildungen in 814 Einzeldarstellungen und 49 Tabellen. Berlin New York Tokyo: Springer-Verlag; 1984. 175 p.

50. Tönnis D, Brunken D. Eine Abgrenzung normaler und pathologischer Hüftpfannendachwinkel zur Diagnose der Hüftdysplasie. Archiv für orthopädische und Unfall-Chirurgie, mit besonderer Berücksichtigung der Frakturenlehre und der orthopädisch-chirurgischen Technik. 1968 Oct 1;64(3):197–228.

51. Connelly A, Flett P, Graham HK, Oates J. Hip surveillance in Tasmanian children with cerebral palsy. J Paediatr Child Health. 2009 Aug;45(7–8):437–43.

52. Bundesärztekammer, Arbeitsgemeinschaft der deutschen Ärztekammern. Leitlinie der Bundesärztekammer zur Qualitätssicherung in der Röntgendiagnostik [Internet]. Bundesärztekammer Deutschland. 50 ff. [cited 2020 Nov 10]. Available from: https://www.bundesaerztekammer.de/fileadmin/user_upload/downloads/LeitRoentgen2008Korr2.pdf

53. Wurzinger LJ. Duale Reihe Anatomie [Internet]. Thieme eRef. Available from: https://eref-1thieme-1de-1z8o2rwtr013b.han.medunigraz.at/ebooks/cs_11350838?fromSearch=true&context=search#/ebook_cs_11350838_cs5534

54. Niethard FU. Duale Reihe Orthopädie und Unfallchirurgie [Internet]. Thieme eRef. Available from: https://eref-1thieme-1de-1z8o2rwtr013b.han.medunigraz.at/ebooks/1945504?fromSearch=true&context=search#/ebook_1945504_SL75755732

55. Child Health BC Hip Surveillance Program. Hip Surveillance Radiographs [Internet]. 2021 [cited 2021 Jul 15]. Available from: https://www.childhealthbc.ca/sites/default/files/Radiology%20Info%20Sheet%20March%202018.pdf

56. Tran BX, Dang KA, Le HT, Ha GH, Nguyen LH, Nguyen TH, et al. Global Evolution of Obesity Research in Children and Youths: Setting Priorities for Interventions and Policies. Obes Facts. 2019;12(2):137–49.

57. Boeyer ME, Sherwood RJ, Deroche CB, Duren DL. Early Maturity as the New Normal: A Century-long Study of Bone Age. Clin Orthop Relat Res. 2018 Nov;476(11):2112–22.